CHAPTER III: BIOCHEMISTRY OF THE ENHANCED BIOLOGICAL PHOSPHORUS REMOVAL SYSTEMS

Zeynep Kisoglu Erdal[1], Clifford W. Randall[1], and Eugene M. Gregory[2]

[1]Civil and Environmental Engineering Department, Virginia Tech, Blacksburg, VA
[2]Biochemistry Department, Virginia Tech, Blacksburg, VA

Abstract

The biochemistry of enhanced biological phosphorus removal (EBPR) has been studied since the mid 1980s by numerous researchers. However, these studies did not make use of powerful biochemistry and chemistry tools, such as enzyme assays and NMR techniques, to explore the metabolism of phosphorus removal under defined conditions. In this study EBPR sludges cultivated in two separate UCT systems operated at 20 and 5°C were used for examination of the anabolic and catabolic reactions taking place during the anaerobic and aerobic stages of phosphorus removal. At both temperatures, glycogen metabolism was shown to be essential for EBPR, and the reducing equivalents for PHA synthesis were obtained through the EMP pathway. Enzyme assays performed on biomass samples indicated that the branched TCA pathway is operative during anaerobic metabolism at 20°C because an excess of NADH is produced during glycolysis. Low temperatures were shown to slow down glycogen metabolism significantly, thereby providing a competitive advantage to poly-P metabolism. At 5°C, the slower glycogen metabolism did not produce an excess of NADH, the branched TCA pathway was not operative, and the pyruvate generated by glycolysis was sent through the glyoxylate cycle under anaerobic conditions. Aerobic metabolism also was investigated, and the glyoxylate pathway was shown to be dominant because it is a good means of conserving carbon by minimizing the CO_2 loss from the system at 20°C. On the other hand, at 5°C, the TCA cycle enzymes were more strongly induced under aerobic conditions. Inhibitor studies were found to be inconclusive because activated sludge has

such a complex extracellular matrix, which reduces the efficiency of inhibitor compounds. Interpretation of such studies must be made with caution. To isolate poly-P metabolism from glycogen, techniques other than enzyme inhibition must be developed.

Keywords: enhanced biological phosphorus removal, biochemical models, PHAs, glycogen, poly-P, intracellular storage, enzyme assays, ^{13}C-NMR, inhibition

INTRODUCTION

Phosphorus is an essential part of the nutrient cycle in nature. It is also essential for growth of the microorganisms in an activated sludge wastewater treatment plant (WWTP), as it makes up 1.5 to 2.0 per cent of the cells. However, due to increasing anthropogenic sources of phosphorus in the environment, it has become a nuisance leading to eutrophication of lakes and deterioration of water quality. Enhanced biological phosphorus removal (EBPR) systems employed as an integral part of the nutrient removal WWTPs successfully remove phosphorus from the incoming wastewaters. Although through practical guidelines EBPR plants are operated smoothly, the microbiology and the biochemistry of the process is not completely understood. Since the 1980s, a great deal of research effort has been dedicated to exploring the underlying mechanisms of EBPR. The current knowledge puts the research community into two camps, if not more: i) followers of the Comeau Model (Comeau *et al*., 1986; Comeau *et al*., 1987; Wentzel *et al*., 1991), and ii) followers of the Mino Model (Mino *et al*., 1987; Liu *et al*., 1996; Maurer *et al*., 1997; Brdjanovic *et al*., 1998; Christensson *et al*., 1998).

As years worth of research revealed, regardless of the stoichiometry, anaerobic PHA storage from feed VFAs occurs in a majority of the cases, and the anaerobic metabolism of the EBPR systems determines the aerobic fate of the intracellular storage polymers. Comeau *et al.* (1986) proposed that the TCA cycle was the source of the reducing

equivalents necessary to reduce acetyl-CoA to PHB. They also suggested that acetate was taken up in its undissociated form (HAc), thereby dissipating the proton motive force (pmf) across the cell membrane, and that the cells had to consume energy from their polyphosphate (poly-P) reserves to maintain a desired proton motive force by expelling protons. Mino *et al*. (1987) studied the effect of poly-P accumulation on acetate metabolism using a sludge acclimated to a feed containing acetate, glucose, and propionate at a range of P/C (mg P/mg C) ratios (0.028, 0.036, 0.064, and 0.084). Also monitoring total carbohydrate (TCH) besides hydroxybutyrate (HB) and phosphate, they observed that TCH was consumed in the anaerobic phase and re-synthesized in the aerobic phase. Hence, they concluded that the intracellular carbohydrate consumption through glycolysis, reflected in the decrease in TCH levels supplies carbon for HB synthesis. Wentzel *et al*. (1991) evaluated the existing biochemical models and suggested a new one called an "Adapted Mino Model". They proposed that the glucose degradation following carbohydrate (i.e. glycogen) breakdown proceeded through the Entner-Doudoroff (ED) pathway, rather than the Embden-Meyerhoff-Parnas (EMP) pathway as originally suggested by Mino and his co-workers. Currently, there are other researchers who support hypotheses built on the ideas of both researchers, such as Pereira *et al*. (1996), Louie *et al*. (2000), and Hesselmann *et al*. (2000).

All of the conclusions of these studies were based on measured quantities of the substrate entering an activated sludge system operated under controlled conditions and the resulting end products of substrate uptake. However, the hypotheses were based on mass balances of substrate-end-product pairs and not based on biochemical monitoring of the sludges under study. Namely, the biochemical mechanisms active under the conditions imposed on the system were not investigated via biochemical methods. Louie *et al.* (2000) employed metabolic inhibitors; malonate, α-ketoglutarate and monofluoroacetate, to probe metabolic pathways. Hesselmann *et al*. (2000) used enzymatic techniques to determine the mechanism of acetate activation to acetyl-CoA. Nevertheless, to move closer to determining a complete picture of EBPR metabolism, further analysis of the enzyme activities is needed.

Apparent involvement of glycogen in EBPR systems has been well documented by numerous researchers as described in the preceding sections. Analyses on EBPR sludge showed that PHA storage concomitant with glycogen consumption under truly anaerobic conditions occur in all EBPR systems. However, the results reported from studies where PHA and glycogen were both measured revealed that the amounts of released phosphorus, produced PHA and consumed glycogen per C-mol of acetate taken up under anaerobic conditions were not constant. This inconsistency may arise because sludges seeded from a different source, and systems operated under slightly different conditions lead to enrichment by a different population dynamic, which consumes and converts the carbon source via different metabolic paths. Thus, what has been observed during years of research was a net result of the concerted and/or opposing activities of different microbial populations.

The following types of microbial activity leading to phosphorus removal are hypothesized to be present in EBPR systems: 1) poly-P is the energy source for SCVFA uptake and its storage as PHA, with reducing power provided from the complete/incomplete operation of TCA cycle; 2) poly-P is the energy source for SCVFA uptake and its storage, with reducing power provided from glycolysis of glycogen reserves; 3) poly-P is the energy source for SCVFA uptake and its storage, with reducing power provided from glycolysis of glycogen reserves and complete/incomplete operation of the TCA cycle; 4) poly-P is the energy source for SCVFA uptake and its storage, with reducing power provided from glycolysis of glycogen reserves and branched operation of the TCA cycle; 5) poly-P is the energy source for SCVFA uptake and its storage, with reducing power provided from the glyoxylate cycle. Glycogen breakdown can proceed via EMP, ED or PP pathways. These pathways converge at glyceraldehyde-3-phosphate to eventually yield pyruvate in all cases, but the amount of reducing equivalents and ATP produced in each pathway is different. Moreover, the branched TCA cycle, complete/incomplete TCA cycle and the glyoxylate pathway all produce succinate that can be converted to propionyl-CoA, the precursor of the HV units. One other pathway that produces propionyl-CoA from pyruvate is the succinate-propionate fermentation pathway (Moat and Foster, 1995). Selection of pathways that will be induced under

anaerobic conditions has a significant impact on the reducing equivalents balance and hence the operation of the enzyme machinery. Furthermore, the amount and composition of the PHA polymer synthesized, and the amount of the glycogen that is consumed depends on the selected pathway.

Operation of all of the above listed pathways is possible under anaerobic conditions, except one. Researchers have been skeptical about complete operation of the TCA cycle under anaerobic conditions, because it is believed that reoxidation of $FADH_2$ produced by the membrane bound succinate dehydrogenase enzyme complex must proceed through the electron transport chain. Thus, it is not widely accepted as possible under anaerobic conditions. On the other hand, under anaerobic conditions, bacteria are known to convert the oxidative TCA cycle into a reductive cycle (Moat and Foster, 1995). The cycle is blocked at α-ketoglutarate dehydrogenase, and it operates as a branched pathway yielding α-ketoglutarate and succinyl-CoA. The complete reductive TCA cycle, which operates in the reverse direction to produce citrate from oxaloacetate also exists in some strict anaerobes, and it is used for CO_2 fixation purposes. Besides, with the presence of the TCA cycle enzymes in the cytosol, bacteria can operate an incomplete TCA cycle under absence of an electron acceptor, to produce succinyl-CoA, which in the end should be consumed to keep the mechanism running without end-product inhibition. This in turn will dictate the PHA-glycogen balance and the PHA composition, as mentioned earlier.

Application of NMR techniques for Investigating EBPR Biochemistry

In the most basic sense, Nuclear Magnetic Resonance (NMR) spectroscopy techniques make use of the fact that when a sample is placed in a magnetic field, the nuclei in the sample molecules generate a bulk macroscopic magnetization (Derome, 1987; Akitt, 1992; Gunther, 1995). Thus, when the system of molecules is disturbed from equilibrium, the response of the system to the disturbance can be a useful tool for the analysis of the identity and the chemistry of the molecules present in the sample. The applied static magnetic field is perturbed by a second magnetic field, which oscillates at

an appropriate radio frequency that in turn creates the NMR spectrum. In a strong magnetic field, the spins of the nuclei tend to align themselves with two energy states: with or against the magnetic field of the NMR instrument. The applied magnetic field will produce an angular acceleration causing the nucleus to precess, like a spinning top, in the direction of the applied magnetic field. When energy is applied at exactly the right frequency, resonance occurs, and the spin flips from one state to the other. As the spins are flipping, they absorb and then radiate energy (Paudler, 1987; Derome, 1987). In order to understand the resonance phenomenon, one can consider a one-dimensional harmonic oscillator. Any oscillator is subject to a restoring force proportional to the displacement, and a friction or damping force proportional to the velocity for the displacement of a unit mass from its equilibrium position by a certain amount. The equilibrium state of the harmonic oscillator occurs when the displacement is zero. When a disturbance to the equilibrium is experienced, the oscillator "relaxes" back to the equilibrium state. The exact frequency of the spin flips identifies the kind of atom that is involved and the other atoms to which it is connected in the molecule. For a given magnetic field strength, each type of nuclear species resonates at a different frequency. By measuring all of the frequencies, the molecular structure can be deduced (Atherton, 1993). The NMR spectrometer detects, amplifies, and displays this action to identify the structure of the molecule. Strong magnetic fields (up to 900 MHz magnets) lead to greater information content and increased sensitivity, allowing the detection and characterization of smaller amounts of material and more complex molecules (Cowan, 1997). Many of the techniques that are valid for the solution state NMR are valid for solid state samples. Like liquid samples, solid state samples are placed in a special sample tube and the tube is placed inside a rotor (Sanders and Hunter, 1993).

Following information gathered from Derome (1987), Kuschel (1989), Akitt (1992), Berliner and Reuben (1992), Atherton (1993), Gunther (1995) and Cowan (1997) is presented since it relates to the ^{13}C chemical shift that was of concern during this study. It is dependent both on the presence of electronegative groups and on the steric environment. Simple interior (primary and secondary) carbons tend to be in the chemical shift range of 25 to 45. Methyl groups which terminate unbranched alkyl chains,

however, are significantly shielded (moved to lower values), as shown by the examples (14, 14.3 and 8.7) (Figure 1).

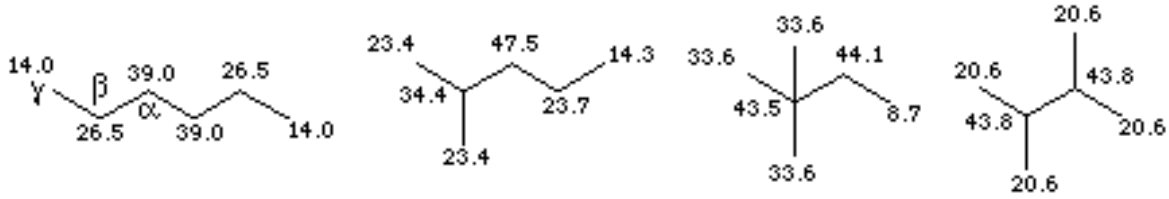

Figure1. Carbon chemical shifts as dictated by the steric environment of each individual carbon atom.

The presence of an electronegative atom such as oxygen tends to move the chemical shift of the carbon down into the region between 65 and 90 (Figure2).

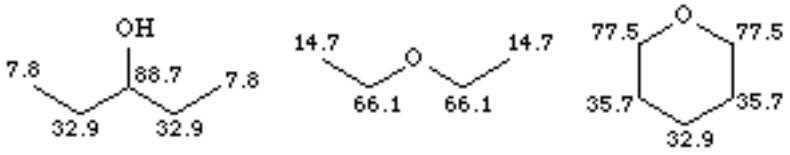

Figure 2. Impact of oxygen atoms in the viscinity of carbon atoms.

Carbonyls are the most highly deshielded carbons which are typically encountered. Their intensity is usually weak, since there are no attached hydrogens. Typical chemical shifts occur in the region between 170 and 210 with esters, carboxylic acids and amides at the low end, and simple ketones and aldehydes at the high end of the range (Figure 3).

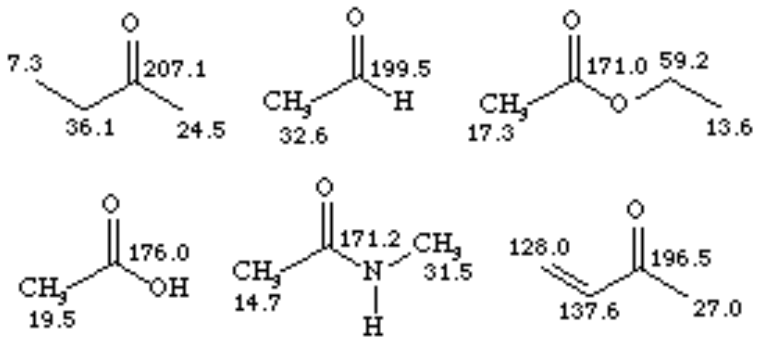

Figure 3. Typical carbon shifts observed in carbonyls in different atomic environments.

Figure 4 gives a summary of carbon-13 chemical shifts given above.

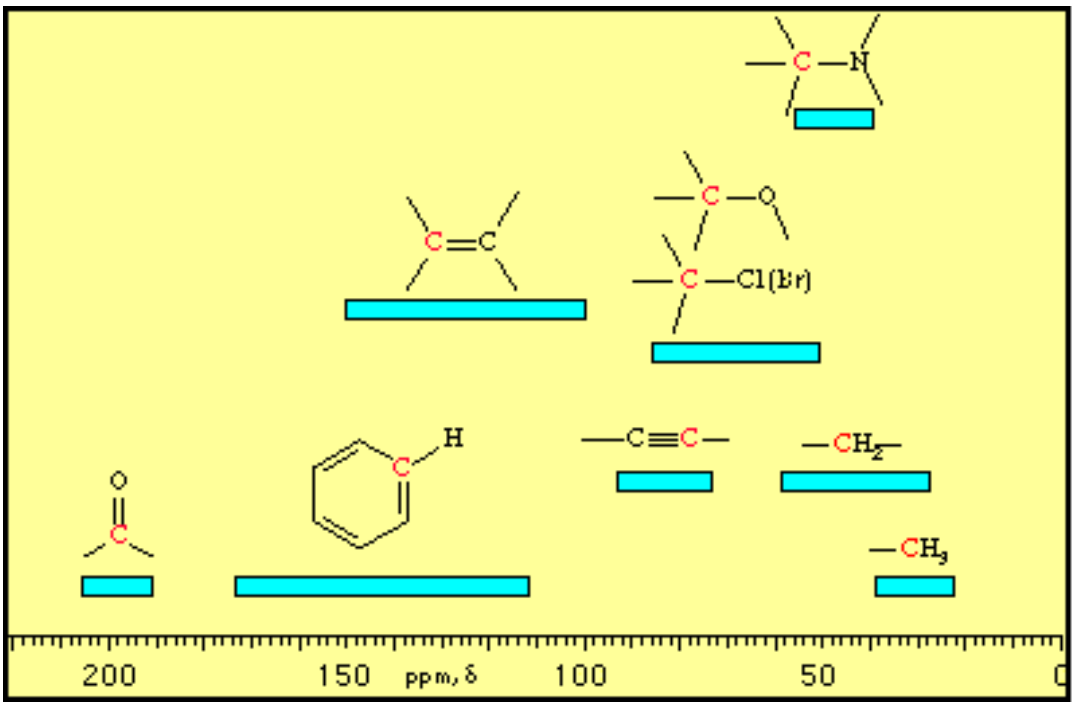

Figure 4. The locations of carbon-13 chemical shifts for different types of organic molecules.

For ^{13}C NMR, simple methyl carbons tend to absorb in the region 15-30, simple methylene carbons are shifted to 20-65, electronegative atoms (oxygen or halogens) move attached carbons to 40-80, alkyne carbons are shifted to 70-90, alkene carbons to 100-150, aromatic carbons to 120-170, and the most highly shifted carbons are generally those of carbonyls, with values of 180-220.

The applicability of solid state NMR techniques to EBPR sludge for the purpose of tracking the changes in the intracellular carbon storage pools requires the physical states of the PHA and glycogen granules within the cell be considered. Glycogen is known to have a highly branched structure that forms compact solid granules. PHAs, on the other hand, are linear chain polymers that have repeating units, and the nature of chemical interactions between neighboring chains would determine the physical state of the polymer. Barnard and Sanders (1989) investigated the PHB granules in a study that employed high-resolution ^{13}C-NMR techniques *in vivo*. Based on the well-resolved spectrum obtained for PHB, they concluded that the growing granules of PHB were in a highly mobile state. Lauzier *et al*. (1992) performed a similar study, which also focused on the crystallization of PHB granules from *Alkaligenes eutrophus*, and their results suggested that removal of water, isolation of the granules from cellular material, and freeze drying induced crystallization. They also showed that the surface of the granules contained an extractable layer of lipids. Based on their TLC results and those of Doi (1990), Lauzier *et al*. (1992) concluded that these lipids forming a bilayer around the granules were principally of glycerol triacetate and glycerol tributyrate. Additionally, they found that growing non-crystalline PHB granules had strongly bound water in their cores that can constitute 5 to 10 % of the polymer weight. Thus, during the biosynthesis of the polymer, water molecules form strong hydrogen bonds with carbonyl groups of adjacent polymer chains, and this bound water keeps the granules in non-crystalline state. Breaking these hydrogen bonds apparently requires high energy. The conclusion from this is that PHA granules can be examined both by *in vivo* and *in vitro* (on lyophilized cellular material) using ^{13}C-NMR techniques.

In EBPR research, the most relevant and recent NMR work done with ^{13}C-labeled acetate fed to EBPR sludge is by Pereira *et al*. (1996) and Maurer *et al.* (1997). The former one is first widely recognized work that goes beyond the boundaries of currently accepted models of Comeau and Mino. They performed an *in vivo* NMR experiment, and based on the appearance of labeled bicarbonate they concluded that the TCA cycle could be operative under anaerobic conditions for their experimental conditions. Maurer *et al.* (1997) on the other hand performed solid state NMR on lyophilized sludge samples, and concluded that the ED pathway was active for the metabolism of glucose units obtained from glycogen stores. As neither work was supported with biochemical studies, their conclusions were based on assumptions made for carbon balance calculations. Pereira and her co-workers acknowledge the possible 30% underestimation of the labeled glycogen carbons, and they account for that underestimation during their calculations. This underestimation is possibly due to the complex polymer structure of glycogen, which makes it a rather solid unit in the cell. The same argument is true for PHA inclusions that are known to go through a crystallization step following polymerization. A transmission electron microscopy (TEM) study performed by Erdal (2002) also clearly showed the individual glycogen particles in the cytosol of cells isolated from EBPR sludge samples. Thus, liquid state NMR is not a suitable tool to work on non-soluble entities present in the cell.

Inhibition of glycogen metabolism

In order to isolate the glycogen-dependent metabolism from others, a series of inhibitors can be used. Glycogen break down and synthesis depend on the relative activities of the glycogen phosphorylase and glycogen synthase enzymes. Inhibition of either break down or synthesis via inhibition of either one of these enzymes can reveal the relationship between glycogen and phosphate pools.

A glucose analogue, 1-deoxynojirimycin (dNOJ), is described as a strong inhibitor of glycogenolysis induced by different external signals including anoxia (Bollen and

Stalmans, 1989). It differs from D-glucose by the presence of nitrogen instead of oxygen for the ring closure and by the absence of oxygen at C-1 (Figure 18). It is widely known as a general potent inhibitor of 1,4-glucosidases. A portion of dNOJ is modified in the cell either by phosphorylation or some other means, and the unmodified dNOJ remains as the probable inhibitor of glycogenolysis (Bollen and Stalmans, 1989). Due to its analogous structure to glucose, dNOJ can be phosphorylated or oxidized at C-6, but not at C-1 because of the absence of the oxygen at that location. They have also shown that of the enzymes that take part in glycogen break down, dNOJ inhibited the α-1,6-glucosidase activity of the glycogen debranching enzyme in hepatocytes.

Dringen and Hemprecht (1993) investigated the effects of 2-deoxyglucose (DG), deoxyglucose-6-P (DG6P), 1,5-gluconolactone (1,5-GL) and 3-ortho-methylglucose (OMG) on glycogen break down. Their results indicate that 1,5-gluconolactone is a strong inhibitor of glycogen phophorylase, but it is not stable after the first hour of the test period. On the other hand, DG, OMG and DG6P were found to be more stable. They also found that after the DG was transported into the astroglial cells, it was converted to DG6P, and it was DG6P that caused the observed inhibition effect. Dringen *et al*. (1993) and Niitsu *et al*. (1999) also used DG and GL as inhibitors of glycogen break down, without any mention or concern about the instability of GL.

One other inhibitor of glycogen phosphorylase is D-gluconohydroximo-1,5-lactone-N-phenylurethane (PUG) (Papageorgiou *et al*., 1989). Its structure, shown in Figure 5, is similar to that of 1,5-GL, but the additional polyurethane group is thought to improve the inhibitory action of PUG that is competitive with G1P, and noncompetitive with respect to phosphate. Because this chemical is not available for commercial purchase, PUG will be considered as an alternative if none of the available inhibitors are found to be effective. The procedure by which it can be manufactured from D-glucose oxime is described in Beer and Vasella (1985). Similarly Watson *et al*. (1994) worked with α- and β-C-glucosides and 1-thio-β-D-glucose compounds for the purpose of designing inhibitors of glycogen phosphorylase system. They based their work on the fact that glucose and glucose derivatives bind to phosphorylase at the catalytic site resulting in a

conformational change that stabilizes the inactive T state of the enzyme and favors phosphatase and glycogen synthase. Producing their own inhibitors, they found that N-methyl-β-glucose-C-carboxamide was the most efficient inhibitor they have tried. In a similar study Martin *et al*. (1991) demonstrated that α-hydroxymethyl-1-deoxyglucose causes an inhibition similar to that of glucose.

On the other hand, oxidized glutathione (i.e. glutathione disulfide; GSSG) was used as a reversible inhibitor of glycogen synthase by Lau and Thomas (1983), Shimazu *et al*. (1978) and Ernest and Kim (1973). The latter group of researchers also looked into the effects of hydroxymercuribenzoate, 5,5'-dithiobis(2-nitrobenzoic) acid (DTNB), iodoacetic acid, iodoacetamide, and N-ethylmaleimide. They observed a concentration and time dependent response from all but the iodoacetic acid. The inhibition by GSSG was pH dependent (best at pH 9.0), and it was reversible by the addition of the reduced glutathione (GSH). They concluded that the inhibition stems from the disulfide exchange reactions between the enzyme and GSSG, and for this reason mercaptoethanol and dithiothrethiol addition to GSSG-enzyme complex fully restored the enzyme activity.

2-Deoxyglucose

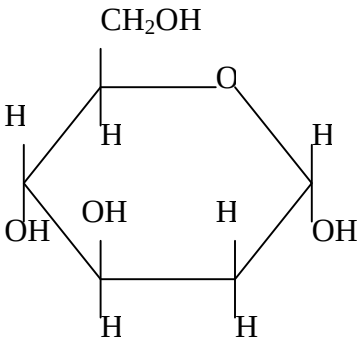

2-Deoxyglucose-6-phosphate

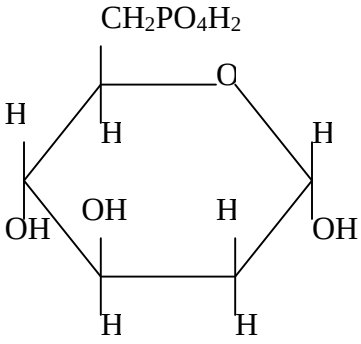

1,5-Gluconolactone

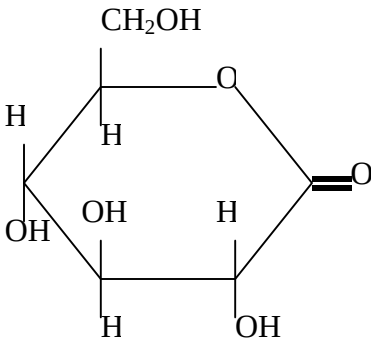

1-Deoxynojirimycin

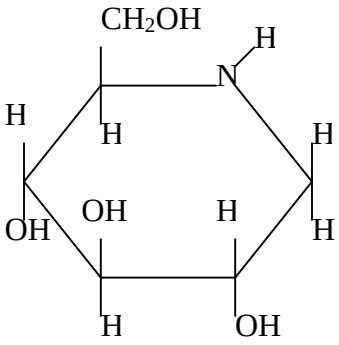

Figure 5. Chemical structures of the inhibitors that will be evaluated.

PUG

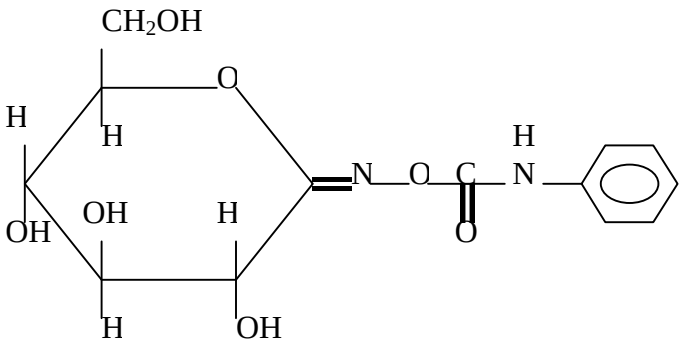

DTNB

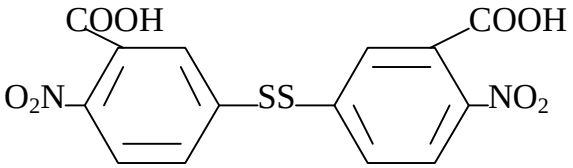

GSSG

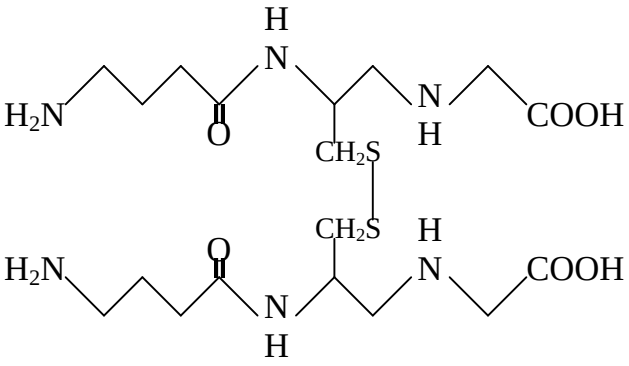

GSH

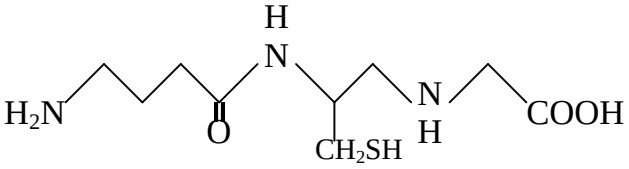

Figure 5. Continued.

Application of Enzymology techniques for Investigating EBPR Biochemistry

Key biochemical pathways of bacterial metabolism may clarify the mechanisms behind EBPR response under different conditions. A versatile tool to examine the operation of pathways is the measurement of enzyme activity. Enzymes are proteins synthesized under conditions which induce the action of the particular enzyme, such as presence or absence of an activator. Enzyme assays are employed to measure specific reactions under controlled conditions.

Although there are methods for measuring enzyme activity in intact cells and in cells that are permeabilized via chemical or enzymatic treatments, most enzyme activity analyses are conducted on cell-free extracts (Gerhadt *et al.*, 1995). One then can use known substrate and cofactor concentrations, coupled assays when needed, and facilitate better control over assay conditions such as pH and ionic strength. Gerhardt *et al.* (1995) lists hydrodynamic shear (French press and Manton-Gaulin homogenizer), ultrasonic cavitation (sonication), grinding with glass beads, and enzymatic lysis (lysozyme with Tris-EDTA addition) as means to disrupt the cell membrane. In this study, sonication was used to obtain crude cell extracts from the mixed liquor samples collected from different reactors of the lab-scale systems. Cell breakage is obtained by the resonation of a transducer that produces movement in a titanium probe tip. This resonation produces sonic waves in the liquid, which then results in formation of a cavitation causing localized high pressure and temperature changes. The sample tube must be placed in ice-NaCl bath to prevent heating of the sample due to the resonating movement of the probe tip. In this study because only comparative enzyme activities are of concern, crude cell extracts instead of enzyme samples purified from mixed liquor samples were assayed. Dialysis of the crude extracts provide removal of low-molecular weight compounds from the extract solution and thereby minimize the possible adverse effects of endogenous substrates and activators already present in the enzyme extract.

Basic Principles of Enzymatic Reactions and Enzyme Kinetics:

Bergmeyer *et al*. (1983a) gives excellent details about enzyme analysis and kinetics of enzymatic reactions. Besides Saier (1987), Kuby (1991), and Silverman (2000), Gerhardt *et al.* (1995) also deals with the practical aspects of the enzyme kinetics, and determination of the kinetic parameters. For the purposes of this study, a brief information on relevant units of quantification in enzymology and enzyme kinetics will be given.

Considering the following equation of a basic enzyme catalyzed reaction, the kinetics of enzyme activity can be depicted.

$$S + E \leftrightarrow ES \rightarrow P + E \qquad (1)$$

where:
S: substrate;
E: enzyme;
ES: enzyme-substrate complex;
P: product

For this catalyzed reaction, the reaction rate is given by the Michaelis-Menten Equation:

$$v = \frac{k_3[E]_0[S]}{(k_2 + k_3)/k_1 + [S]} = \frac{k_{cat}[E]_T[S]}{Km + [S]} = \frac{v_{max}[S]}{Km + [S]} \qquad (2)$$

where:
v: observed velocity

$k_{1,2,3}$: rates of the forward (2 and 3) and backward (1) reactions.

Km: Michaelis constant of the substrate

V_{max}: velocity attained at a vast excess of substrate; μmole mL^{-1} min^{-1} (or, units per mL)

$[E]_T$: total concentration of the enzyme; μmole mL^{-1}

k_{cat}: molecular activity of the enzyme; min^{-1}

Determination of the values of the kinetic constants is essential for designing enzyme assays. However, in this study published assay protocols were used, and thus the kinetic rates for each enzyme under study were not determined. Nevertheless, the information provided above was useful in understanding the assay protocols and interpreting the results of the enzyme assays that were performed.

As presented by Gerhardt *et al*. (1995), before an assay procedure is employed for sample analysis, the procedure itself must be tested for accuracy and reproducibility of data. First, the assay must demonstrate linear dependence of velocity on the amount of enzyme added. For this purpose, the assays were tested using commercially available enzyme during the study. Different quantities of the native enzyme were introduced to the assay mixture and the resulting reaction rates were evaluated for linear dependence between the enzyme concentration and the reaction rate. Also the rate reading were taken at the period where substrate consumption, or product formation with respect to time is constant. This period was early in the assay so that the substrate depletion or product accumulation would be minimal. A number of reasons for departure from linearity at excessively high reaction velocity are significant substrate depletion, reversibility or inhibition due to product accumulation, and pH changes in inadequately buffered reactions which produce or consume protons. Appropriate dilution of the enzyme mixture was used for high velocity reactions. Finally, negative and positive controls were used to test the suitability of the assay protocol. Negative control is when the enzyme mixture is replaced with the appropriate buffer solution, to control whether the assay mixture itself gives a reaction rate without the presence of the enzyme under study. One other form of negative control is the substitution of the enzyme's substrate with buffer solution to test for the presence

of an endogenous substrate in the crude enzyme extract. A positive control is when the enzyme extract sample is replaced with the native enzyme, to test for the suitability of the assay conditions. In summary, the linear portion of the d[S]/dt or d[P]/dt curve was utilized for rate calculations, after the assay was shown to be reliable. The slope of the tangent to the curve at time zero for reactions that lack a zero-order portion could also be used.

Under some circumstances, coupled assays are utilized instead of one step, straightforward assay protocols. The measurement of reaction products is made easier by the introduction of an auxiliary enzyme, which converts the primary product to a new compound that will provide a reliable detection. There are three requirements for a coupled assay to yield valid measurements: first reaction must be first order, second reaction must be first order, and neither one of the reactions must be reversible. These conditions ensure that the product of the first reaction will be in constant supply for the second reaction to go forward.

Because the assay conditions such as pH, buffer type, ionic strength, concentrations of reactants and cofactors and assay temperature have great bearing on the results of an assay, they must always be reported, and unless they are known, values from different studies cannot be compared. Assay temperature is especially important, as it can drastically change the reaction rate. Enzyme assays are usually performed at “optimum” temperatures determined for each enzyme. Another factor that alters the reaction rates is the presence of an endogenous substrate in the crude extract as mentioned earlier. Especially when the enzyme activity is moderately low and the extract cannot be diluted significantly, the contaminating effect of he endogenous substrate will be important. This problem can be overcome by using saturating substrate concentrations. Activators present in the crude extract can also lead to nonlinear plots, and this factor may not be overcome even at saturating substrate concentrations. In the case of endogenous substrates, when the actual substrate is omitted, there will still be a reaction velocity, and it will interfere with the rate determination, and kinetic analysis using these rates must

not be performed. In this case, in order to eliminate such contamination dialysis at 4°C in SOD buffer was performed before the crude extracts are used for assay purposes.

For all the enzyme assays that were performed during this study, a Shimadzu UV/VIS recording spectrophotometer was used. The theory behind the absorption photometry is also given in Bergmeyer *et al*. (1983a), and it will be briefly summarized here to establish the basis for the calculation of the enzymatic reaction velocity values from the absorbance change measured on the spectrophotometer.

The fundamental principle of the spectroscopy relies on the Bouguer-Lambert-Beer Law, which applies only to highly dilute solutions:

$$A = \varepsilon \; x \; c \; x \; d \qquad (3)$$

where:

A: absorbance; dimensionless

c: concentration of the absorbing substance; mol L^{-1}

d: path length of the light; mm

ε : molar decadic absorption coefficient that yields an absorbance of 1.0 at a fixed wavelength and a path length of 10 mm; L mol^{-1} mm^{-1}

In order to be able to calculate the change in substrate/product concentration with respect to time, following equation will be used:

$$\frac{A}{t} = \varepsilon \times d \times \frac{c}{t} \qquad (4)$$

where c/t will have the units of mol L^{-1} min^{-1}.

As discussed earlier, there are a number of biochemical pathways common to most living organisms, e.g. TCA cycle, EMP, ED, Pentose Phosphate, and glyoxylate pathways. Another possible anaerobic pathway is the succinate-propionate pathway of *Propionibacterium* and similar groups of propionate bacteria (Moat and Foster, 1995). In this study, mass fluxes between different storage pools and active enzyme systems of an EBPR sludge strongly enriched with a poly-P storing community was examined for the purpose of understanding the underlying biochemical interactions. The above listed pathways were considered during the evaluation of the results of the NMR analysis and the enzymatic activity tests.

MATERIALS AND METHODS

A UCT configuration BNR lab-scale system consisting of two 2-L anaerobic, two 2-L anoxic and three 3.5-L aerobic completely mixed reactors (Figure 6a) was operated in a constant temperature room kept at 20±1°C. The mean cell residence time (MCRT) of 10 days was used throughout the study. Synthetic feed flow rate was set to 35 L/day, resulting in nominal hydraulic residence times (HRTs) of 2.7 hours anaerobic, 2.7 anoxic, 7.2 aerobic and 12.7 hours total. Internal system recycles; i.e. nitrate recycle from third aerobic reactor to first anoxic reactor, return activated sludge to first anoxic reactor, and anoxic recycle from second anoxic reactor to first anaerobic reactor were maintained at 42 L/day. All the flow rates were measured and recorded frequently, especially on the days of sludge sampling. This ensured accuracy of the mass balance determinations performed on system parameters such as PO_4-P, PHA and glycogen, since the peristaltic pump rates would vary +/- 2 to 3 L/day in the long run. An A/O configuration lab-scale system (Figure 6b) was also operated in the 20°C constant temperature room, and it was fed and maintained similar to the UCT plant. Its synthetic feed flow rate was set at 27 L/day, and the return activated sludge (RAS) rate was 36 L/day.

Air diffuser stones and aquarium pumps were used for both aeration and mixing purposes in the aerobic zones of the systems. Non-aerated zones of the systems were mixed with motors installed at the top of each reactor. Seed sludge was obtained from Roanoke City Wastewater Treatment Plant, Virginia. An MCRT of 10 days was maintained through solids wastage from the last aerobic reactors. Feed water prepared daily was deoxygenated by purging with N_2 gas until the dissolved oxygen concentration in the influents, which entered the systems through the first anaerobic reactors, fell well below 1 mg/L. Synthetic feed was prepared to contain acetate as the sole COD and VFA source, 30 mg/L N added as $(NH4)_2SO_4$, K_2HPO_4, 125 mg/L $CaCO_3$ alkalinity as $NaHCO_3$, 210 mg/L $MgSO_4$, 44.4 mg/L $CaCl_2$, 1.11 mg/L $FeCl_3$, 0.66 mg/L $MnCl_2 \cdot 6H_2O$ 0.44 mg/L $ZnSO_4 \cdot 7H_2O$, 0.14 mg/L $CuSO_4 \cdot 5H_2O$, 0.14 mg/L $CoCl_2 \cdot 6H_2O$, 0.05 mg/L KI, 0.12 mg/L H_3BO_4. Influent PO_4-P concentration was kept constant at 20 mg/L by preparing the PO4-P feed separate from the COD feed to minimize decreases of both acetate and PO4-P during the daily feed cycle. A constant PO_4-P pump rate was also maintained to assure a constant combined feed P concentration.

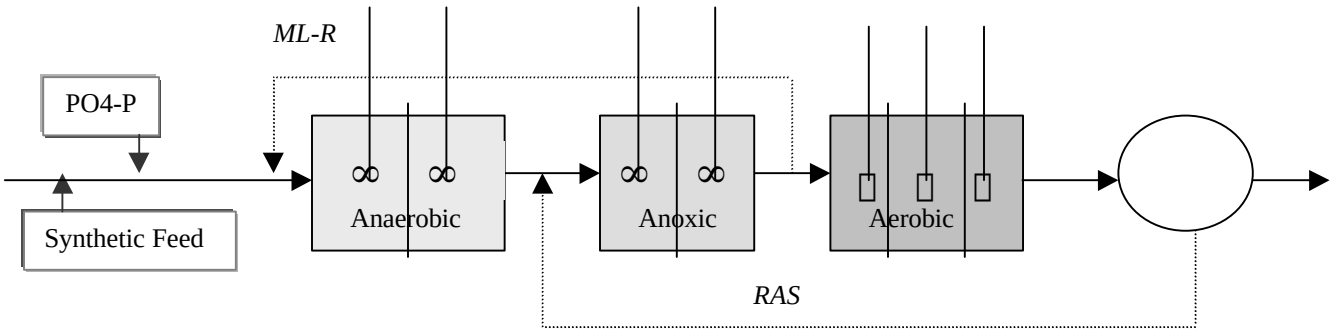

Figure 6a. UCT configurations lab-scale system operated during the study

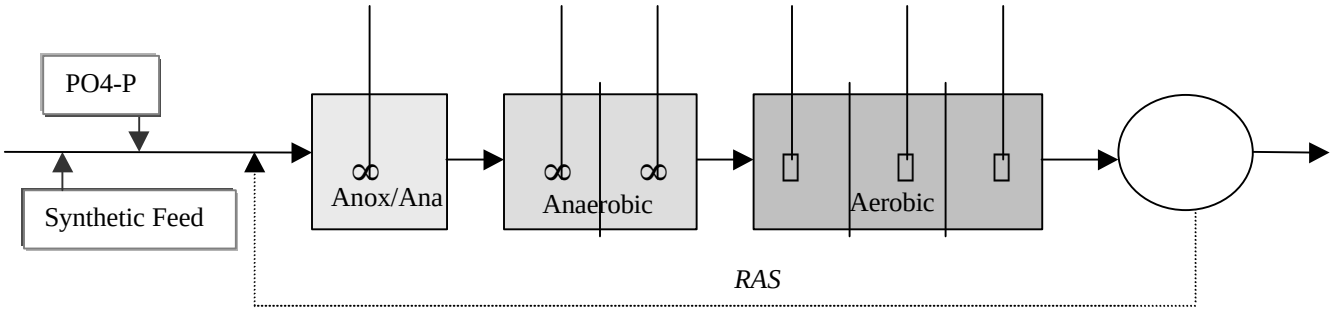

Figure 6b. A/O configuration lab-scale system operated during the study

The systems were operated for three months after they were placed into operation before steady state was assumed and data collection started. The plants were monitored for 1.5 years thereafter, through the measurement of soluble and total COD, MLSS, MLVSS, NO_3^--N, NO_2^--N, NH_4^+-N, PO_4^{-3}-P, OUR, PHB, PHV, and glycogen on samples taken from the influent, each of the reactors, the recycle lines, and the system effluent.

In the anaerobic-aerobic batch tests performed, aerobic sludge taken from the last aerobic reactor was supplemented with a small volume of synthetic feed solution, which contained acetate, ammonia-N and PO4-P. Anaerobic conditions were initiated and maintained by continuous N_2 sparging. Sampling was performed through tubing by suction with a peristaltic pump. At the end of the anaerobic period, air was introduced to establish aerobic conditions. Mixed liquor samples collected for enzyme assays were taken from the anaerobic and aerobic zones of the systems operated at 20° and 5°C, and they were instantly frozen in liquid N_2.

The cation and anion analyses of filtered samples were performed using a DIONEX DX-120 ion chromatograph equipped with anion and cation columns according to APHA (1995). The system has an attached autosampler that can switch between separate anion and cation runs. SCOD, MLSS and MLVSS were also analyzed as outlined APHA (1995).

For the analysis of the internal storage products glycogen, PHB and PHV, mixed liquor samples were centrifuged for 5 minutes at 10 000*g*, the supernatant was removed, and the remaining solids were instantly frozen in liquid N_2 to prevent any further changes. Frozen sludge samples were lyophilized. Treatment of the lyophilized solid samples for the quantification of PHAs was done according to Punrattanasin (2001); however a different GC column that was more sensitive to lipids, and a preset oven temperature program were utilized. Accordingly, dried solid samples were weighed into 5-mL high pressure Wheaton V-vials. Eight to ten external PHA standards were prepared by weighing different quantities of (0 to 15 mg) PHB-HV copolymer standard (12%HV) obtained from Sigma Chemicals. Methanol-sulfuric acid-benzoic acid solution was added (2 mL) to each vial. Benzoic acid served as an internal standard, and the solution was prepared freshly by solubilizing 50 mg of benzoic acid in 100 mL of 3% sulfuric acid in a methanol solution (v/v). Before vials were tightly sealed, 2 mL of chloroform was also added to each vial. The vials were then incubated in an oven at 100^{o}C for 3.5 hours. Following digestion, the vials were cooled to room temperature and 1 mL of distilled water was added to each vial. The vials were shaken for 10 minutes to separate methanol and chloroform layers. A sufficient volume of the chloroform phase (~1 mL) was transferred into GC autosampler vials using Pasteur pipettes. The samples were injected automatically to a HP gas chromotograph equipped with an autosampler, a Carbosieve column and a FID detector. The injector and detector temperatures were 160 and 200°C, respectively. The temperature program used for the oven was: the starting temperature was 90°C (4min), the temperature was ramped up to 130°C (6°C per min), and kept there (6 min).

Glycogen measurements were performed according to a modification of the method outlined by Gerhardt *et al.* (1995). Glycogen is resistant to hydrolysis in alkali, but it is readily soluble in water and acid, and insoluble in ethanol. Lyophilized biomass solid samples were weighed into screw-capped centrifuge tubes and 1 to 2 mL of 30% wt/vol KOH was added depending on the quantity of the solids. The samples were digested at 100ºC for 3 hours to break down the cells and to solubilize the glycogen homopolymer. After 3 hours, the samples were taken out and cooled to room temperature. Then, to each tube water (3mL) and ice-cold ethanol (8 mL) were added to precipitate the glycogen. The opaque solution formed after addition of ethanol was centrifuged for 15 min at 10,000*g*. The pellet was washed with 60% (vol/vol) ice-cold ethanol. The remaining precipitate was dried at 60ºC. The pellet was digested at 100ºC in 3 mL of 6N HCl for 1 hour to convert the glycogen to glucose. Glucose was measured using the Phenol method (Gerhardt *et al*., 1995). Glycogen content was then reported as mg glucose per mg of dry solids.

InhibitionStudies

The inhibitors that were meant to be used for inhibition and isolation of glycogen metabolism in the EBPR sludges were screened using a series of batch tests. The following inhibitors were evaluated:

- 1-deoxynojirimycin
- 2-deoxyglucose
- deoxyglucose-6-P
- gluconolactone
- 3-ortho-methylglucose
- glutathione
- 5,5’-dithiobis(2-nitrobenzoic) acid
- iodoacetic acid

N-methyl-β-glucose-C-carboxamide, α-hydroxymethyl-1-deoxyglucose, and D-gluconohydroximo-1,5-lactone were left out because of economic reasons. They were not commercially available, and would have required special synthesis at the Chemistry Department of Virginia Tech.

The inhibitor concentrations were selected to be a minimum of ten fold higher then those used in the referenced studies. Those studies were performed either with pure enzyme samples or with isolated cells. Since the penetration and uptake of the inhibitor molecules through the bulk structure and exocellular polymers of EBPR sludge and into the individual cells was of concern, higher concentrations were used. The concentration of the mixed liquor solids was around 1000mg/L during these tests. Some of the inhibitors were tested against a control only twice due to economic considerations.

The results of this preliminary experimentation step revealed one potential inhibitor that may be applied to an EBPR system (gluconolactone). However, the concentration at which it was effective made it unrealistic to apply to a lab scale EBPR unit to be monitored over a reasonable time period. Hence, any further use of the inhibitor was stopped. The results of the inhibitor experiments are illustrated by Figures 10-13.

Enzyme Assays:

Samples were prepared as discussed previously. Microbial cells were disrupted via sonication (cavitation) according to Gerhadt *et al.* (1995) for 8 minutes. The sonicator was operated at 5 sec cycle time and at a 60% duty cycle, with sample cooling with a NaCl-ice bath. Following sonication, the biomass samples were centrifuged at 12,000*g* for 15 min. The supernatant was then dialyzed in buffer (50 mM potassium phosphate, 1 mM EDTA; pH 7.8) at 4°C overnight. Dialyzed samples were again centrifuged at 12,000*g* for 15 min, and the supernatant was preserved in the freezer until assayed.

Enzyme assays were performed to evaluate the activities of selected metabolic pathways using a Shimadzu UV/Vis recording spectrophotometer.

Fumarate Reductase: Lemire and Weiner (1986) summarized the fumarate reductase metabolism of *E. coli* grown anaerobically on glycerol-fumarate medium. Fumarate serving as the terminal electron acceptor helps the organism grow on a non-fermentable carbon source in the absence of oxygen. Fumarate reductase is an "intrinsic membrane enzyme" with it catalytic site exposed to the cytosol. Assay solutions and method are as follows:

1. Sodium phosphate, 200 mM (pH 6.8); dithiothreitol, 0.5 mM
2. Benzyl viologen, 2.5 mg/mL, in H2O
3. Sodium dithionite, 20 mM, in 200mM sodium phosphate, pH 6.8. The solid dithionite was stored desiccated until used. Solutions were prepared fresh hourly and stored in closed containers with very little air space. To prevent immediate oxidation of dithionite, the method was slightly modified to include a step where the air in the vial containing the dithionite was replaced with Argon. In spite of this, dithionite was stable for 1.5 hours at most.
4. Sodium fumarate, 500 mM (pH 7.0)

Fumarate reductase activity was followed by measuring the initial rate of fumarate-dependent oxidation of reduced benzyl viologen at 570 nm (molecular extinction coefficient = 7800). The assay was carried out in open 3-mL plastic cuvettes at 24 C. According to Lemire and Weiner (1986) control assays performed under N_2 atmosphere in Thunberg cuvettes give essentially identical results. The standard assay mixture contains 2.5 mL of solution 1, 0.1 mL of solution 2, 0.09 mL of solution 3, and enzyme (1-50 μL). All reagents except the fumarate are added to the cuvette, which is gently inverted twice. Upon addition of 0.1 mL of solution 4, the decrease in absorbance is followed as a function of time. In the absence of fumarate, the dithionite should be sufficient to maintain a constant absorbance for 3 – 4 minutes. Activities are expressed as micromoles of reduced benzyl viologen oxidized per minute.

***Methylmalonyl-CoA decarboxylase*:** Activity was assayed according to Bermudez *et al*. (1998) by measuring the formation of propionyl-CoA by HPLC. The reaction mixture contained the following in a total volume of 0.50 mL:

1. 1 mM dithioerythritol
2. 0.3 mM methylmalonyl-CoA
3. 10 mM citrate-phosphate buffer (pH 6.5)
4. Enzyme/sample

The reaction was initiated by the addition of methylmalonyl-CoA, and the reaction mixture was incubated at 30°C for 60 minutes. The reaction was stopped by addition of 10 μL of 6 N perchloric acid. Precipitated protein was removed by centrifugation at 12,000 x *g*. The supernatant was filtered through a 0.22 μm pore size membrane filter and used for HPLC chromatography. Activity is expressed as picomols of propionyl-CoA formed per minute per mg protein. A C-18 HPLC column was used for the measurements. The mobile phase flow-rate was 1 mL per min. For the sample detection at 254 nm, Eluent A was a 50 mM sodium acetate buffer at pH 5, and Eluent B was acetonitrile (97:3).

Methylmalonyl-CoA mutase: The activity was investigated according to Bermudez *et al*. (1998) by measuring the methylmalonyl-CoA formed by HPLC. The reaction mixture contained the followings in a total volume of 0.50 mL:

1. 1 mM dithioerythritol
2. 0.5 mM succinyl-CoA
3. 60 μM coenzyme-B_{12}
4. 100 mM Tris-HCl buffer (pH 8.0)
5. Enzyme/sample

The reaction was initiated by the addition of succinyl-CoA, and the reaction mixture was incubated in the dark at 30°C for 30 minutes. The reaction was stopped by the addition of 20 μL of 6 N perchloric acid. Precipitated protein was removed by centrifugation at 12,000 x *g*. The supernatant was filtered through a 0.22 μm pore size membrane filter and used for HPLC chromatography. Activity is expressed as picomols of methylmalonyl-CoA formed per minute per mg protein. The HPLC column used for the measurements was a C18 column. The mobile phase flow-rate was 0.5 mL per min. For the sample detection at 254 nm, Eluent A was a 50 mM sodium acetate buffer at pH 5, and Eluent B was acetonitrile (97:3).

Isocitrate lyase: The authors Popov *et al.* (1996); Popov *et al.* (1996); and Serrano *et al.* (1998) all refer to Dixon and Kornberg (1959) for the assay of isocitrate lyase, one of the key enzymes of the glyoxylate cycle. The assay was performed in a 3 mL mixture of the following reagents:

1. 50 mM Tris-HCl buffer at pH 7.5
2. 2 mM isocitrate
3. 5 mM $MgCl_2$
4. 4 mM phenylhydrazine

The formation of glyoxylate phenylhydrazine is followed spectrophotometrically at 324 nm. The molar extinction coefficient is 1.67×10^4 $M^{-1} cm^{-1}$.

Malate synthase: The other key enzyme of the glyoxylate cycle, malate synthase was assayed in 3 mL reaction mixtures of following composition (Popov *et al*., 1996; Popov *et al*., 1996; Serrano *et al*., 1998):

1. 50 mM Tris-HCl buffer (pH 7.6)
2. 0.15 mM acetyl-CoA
3. 2 mM glyoxylate
4. 1 mM 5,5'-dithio-*bis*(2-nitrobenzoic acid) DTNB

The enzyme activity based on the formation of 5-mercapto-2-nitrobenzoic acid was measured at 412 nm using an extinction coefficient of 1.36×10^4 M^{-1} cm^{-1}.

-Ketoglutarate dehydrogenase: The enzyme activity was assayed according to Monori *et al*. (1985) and Lai and Cooper (1986) by measuring the initial rate of increase in absorbance at 340 nm on a recording spectrophotometer. The 3 mL reaction mixture contained

1. 100 mM Tris-HCl buffer (pH 7.5)
2. 5 mM 2-mercaptoethanol
3. 10 mM $MgCl_2$
4. 2 mM thiamine pyrophosphate
5. 1 mM sodium α-ketoglutarate
6. 1 mM NAD^+
7. 0.2 mM CoA
8. Enzyme/sample

α-Ketoglutarate was pipetted into the reaction mixture before the addition of the enzyme source. The reaction was then started by addition of CoA.

Phosphofructokinase: The enzyme activity is measured according to UNITIKA Enzymes suggested methods, through a coupled assay that results in oxidation of NADH, using the following solutions at indicated volumes were in a final volume of 3 mL:

1. 2.74 mL, 0.1 M Tris-HCl (pH 9.0)
2. 0.03 mL ATP solution, 100 mM (0.605 g ATP disodium salt·$3H_2O$/(8.2 mL distilled water + 1.8 mL 1N NaOH)
3. 0.04 mL of phosphoenolpyruvate (PEP) solution, 56 mM (0.15 g PEP-MCA salt/10 mL distilled water)

4. 0.06 mL of NADH solution, 13.1 mM (0.10 g NADH disodium salt·$3H_2O$/mL distilled water)
5. 0.06 mL of fructose-6-phosphate (F6P) solution, 500 mM (1.55 g F6P disodium salt / 10 mL distilled water)
6. 0.006 mL of KCl solution, 2.5 M (16.64 g KCl/100 mL distilled water)
7. 0.06 mL of MgSO4 solution, 100 mM (2.47 g MgSO4·$7H_2O$ /100 mL distilled water)
8. 0.003 mL of pyruvate kinase (PK), (10,000 U / 2.5 mL)
9. 0.006 mL of lactate dehydrogenase (LDH), 550 U / mL)

Cuvettes with the assay mixture were incubated at 30°C for 3 minutes. Enzyme solution or the sample was added to start the reaction. Absorbance change at 340 nm was recorded, and the reaction rates were calculated from the linear portions of the curves.

Malate dehydrogenase: The enzyme activity was assayed according to the following protocol:

1. NAD^+; 15 mM – 100 mL
2. L-malate; 0.49 M – 200 mL
3. PMS; 25 mM – 30 mL
4. MTT; 5 mM – 250 mL
5. Buffer (PO_4)– 2.32 mL
6. Enzyme extract; 0.10mL

Absorbance change at 578 nm was recorded, and the reaction rates were calculated from the linear portions of the curves.

Isocitrate dehydrogenase: The enzyme activity was assayed according to the following protocol:

1. NAD^+; 15 mM – 0.10 mL
2. Isocitrate; 2 mM – 0.20 mL

3. PMS; 25 mM – 0.03 mL
4. MTT; 5 mM – 0.25 mL
5. Buffer (PO_4)– 2.32 mL
6. Enzyme extract; 0.10mL

Absorbance change at 578 nm was recorded, and the reaction rates were calculated from the linear portions of the curves.

Glucose-6-phosphate dehydrogenase: Enzyme activity was determined using an assay mixture at the following composition:

1. Buffer; 0.1 M Tris-HCL (pH 9.0) – 2.54 mL
2. NADP+; 22.5 mM - 0.12 mL
3. Glucose-6-phosphate; 33 mM - 0.24 mL

Cuvettes with the assay mixture were incubated at 30°C for 3 minutes. 0.10 mL of enzyme solution or the sample was added to start the reaction. Absorbance change at 340 nm was recorded, and the reaction rates were calculated from the linear portions of the curves.

Protein Measurements

Bicinchoninic acid (BCA) method was used for the protein measurements in crude cell extracts that were used for the enzyme activity measurements. Bovine serum albumin (BSA) protein was used to construct the standard curves. 0.1 mL of sample (3 different dilutions per sample) or standards were pipetted into protein-free test tubes, and to this 2 mL of the working reagent (50 mL BCA and 1 mL 4%$CuSO_4$) was also added (Pierce Chemical Co.). The contents were mixed well, and then incubated on a shaker table for 30 minutes at 37°C. At the end of the incubation time, the tubes were cooled to room temperature, and the absorbance of each standard and sample was measured at 562 nm.

The protein content of each sample was calculated from the standard curve. These values were used in the specific enzyme activity calculations.

Data analysis and statistical comparison

The number of samples was selected as large as possible to provide better data quality. The standard error of the means of the measured parameters were calculated and reported wherever necessary, unless otherwise mentioned. The standard error of the means was also used during the estimation of error bars presented in the figures.

***Solid State NMR analysis*:**

Since the major concern of this research was the examination of the carbon budget as observed in EBPR systems, ^{13}C-NMR was used to monitoring the changes in carbon species as they took place in EBPR sludges when exposed to non-oxic followed by oxic periods. For this purpose, aerobic sludge taken from the 20ºC UCT plant was exposed to anaerobiosis under the presence of ^{13}C-labelled acetate (0.712 mmoles of labelled carbon per 150mL mixed liquor, 6000 mg MLSS/L; 65%VSS) for two hours by sparging N_2-gas, followed by a four-hour aerobic period where air was introduced by small aquarium pumps. At the end of first aerobic period, sludge was allowed to settle, the supernatant was removed and replaced with synthetic feed that contained the same quantity of non-labeled acetate. Sludge was exposed to the same sequence of non-oxic followed by oxic periods. Sludge samples were collected at the beginning, middle and end of each period, and the samples were immediately frozen in liquid nitrogen to preserve the state of each carbon pool. Prior to further analysis samples were lyophilized. Samples were analyzed with a Bruker Model MSL-300 (75 MHz ^{13}C) at the NMR facility of the Chemistry Department of Virginia Tech. Adamantane was added to each solid sample as an internal standard. NMR spectra were obtained with 2 hour runs. Each run consisted of 800 scans, with 10 second delay and 35 degree pulse, using the Bloch decay method. Data

acquisition and analysis were performed using the NUTS NMR offline data processing software, and ACD/Labs software suite was used for carbon spectra calculations for PHA and glycogen polymers.

A similar test was performed at 5ºC, using the EBPR sludge (4400 mg/L MLSS, 47% VSS) that was acclimated and maintained at 5ºC for approximately 1 year. Considering the slow kinetics of acetate uptake and enzymatic reactions at this temperature, an anaerobic period of 7 hr was used, and the following aerobic period was 14 hr. In order to obtain better peak quality, the quantity of the labeled carbon was increased 45% to 1.5 mmol per 250 mL, which corresponds to 400mgAc/L. At the end of the 24-hr period, sludges were left to settle, and the supenatants were replaced with the same volume of non-labeled acetate solution (400 mg/L). The second anaerobic-aerobic cycle also took 24 hr. Intermediate samples were analyzed for PO_4-P, NO_3-N, Acetate, PHAs and glycogen. NMR spectra were obtained with 1 hour runs. Each run consisted of 300 scans, with 10 second delay and 35 degree pulse, using the Bloch decay method. Adamantane was not used due to its interference with C-2 of PHA which comes out at 42ppm.

RESULTS AND DISCUSSION

The ostensible dependence of enhanced biological phosphorus removal on glycogen metabolism was shown to be true by Erdal and Randall (2002b). In this study, a detailed investigation of the underlying mechanisms of the relationship between the intracellular storage pools and EBPR behavior will be presented. For this purpose, performance data from the UCT and the A/O systems were evaluated and the biomasses in both systems were subjected to a number of analyses. The performance data for the A/O system maintained at 20°C is presented in Table 1. Figures 7 through 9 present the calculated mass balance values for phosphate, PHA and glycogen.

The A/O system consistently removed all of the influent phosphorus, which averaged 25 mg/L as phosphorus. The system was operated under near constant PO_4-P feed concentration without any emphasis given to determining the maximum removal capacity of the system. The cultivated sludge had 20% HV production under anaerobic conditions, which was similar to that of the 20°C UCT system. The average observed phosphorus removal in the UCT system was 24 mg/L when the nitrate recycle was in operation, and it was 42 mg/L when the recycle was shut off for experimental purposes.

The data plotted in Figures 7-9 indicate that phosphorus release was very rapid and nearly all of it occurred in the first anaerobic reactor, but PHA synthesis and glycogen utilization occurred more slowly, and could be reasonably described by a first order reaction. The implication is that PHA synthesis was more closely related to the rate of glycogen utilization than to the rate of phosphorus release. This is probably because PHA synthesis requires reducing equivalents, and these reducing equivalents are provided by glycogen degradation. Consequently, the rates of these two reactions are very interrelated. On the other hand, once the acetate is taken into the cells, its activation into acetyl-CoA requires ATP, which can be rapidly provided by poly-P breakdown, which results in rapid release of phosphate.

The remarkable aspect of the aerobic results is that glycogen was re-synthesized so rapidly. About 80% of the total amount re-synthesized in the aerobic zone was accomplished in the first aerobic reactor. On the other hand, PHA utilization and phosphate uptake were more evenly spread throughout the aerobic zone, and paralleled each other, confirming that phosphate uptake requires PHA utilization.

Table 1. Average performance values for the A/O system; value±S.E.M.

Inf COD mg/L	Inf PO4-P mg/L	Inf NH4-N mg/L
440±7	25±2	29±2

	AN1	AN2	AN3	AE1	AE2	AE3	EFF	RAS
PO4-P[1] mg/d	-5672±208	-345±68	-224±103	4729±289	1548±121	557±97		
HB[2] mg/d	4386±332	2001±257	1393±210	-4498±540	-1722±165	-1213±127		
HV[2] mg/d	737±59	415±106	450±89	-908±140	-399±49	-280±94		
HA[2] mg/d	4865±366	2454±345	2065±294	-5407±407	-2095±218	-1521±181		
GLY[3] mg/d	-2522±446	**-1358±209**	-1054±**257**	7833±**1376**	1459±1368	143±184		
OUR mg/L/hr				102±10	41±5	31±4		
MLSS mg/L	3367±181	3789±159	4012±194	4707±123	4454±201	4583±214	81±8	5054±385
MLVSS mg/L	2440±133	2798±194	2910±144	3275±112	2940±121	3097±159	56±5	3423±263
%VSS	0.72±0.01	0.72±**0**	0.73±0.01	0.69±0.01	0.67±0	0.67±0.01	0.72±0.01	0.68±0.01

[1]Negative values indicate phosphate release, and positive values indicate phosphate uptake.

[2]Negative values indicate consumption, and positive values indicate storage.

[3]Negative values indicate glycogen utilization, and positive values indicate glycogen re-synthesis.

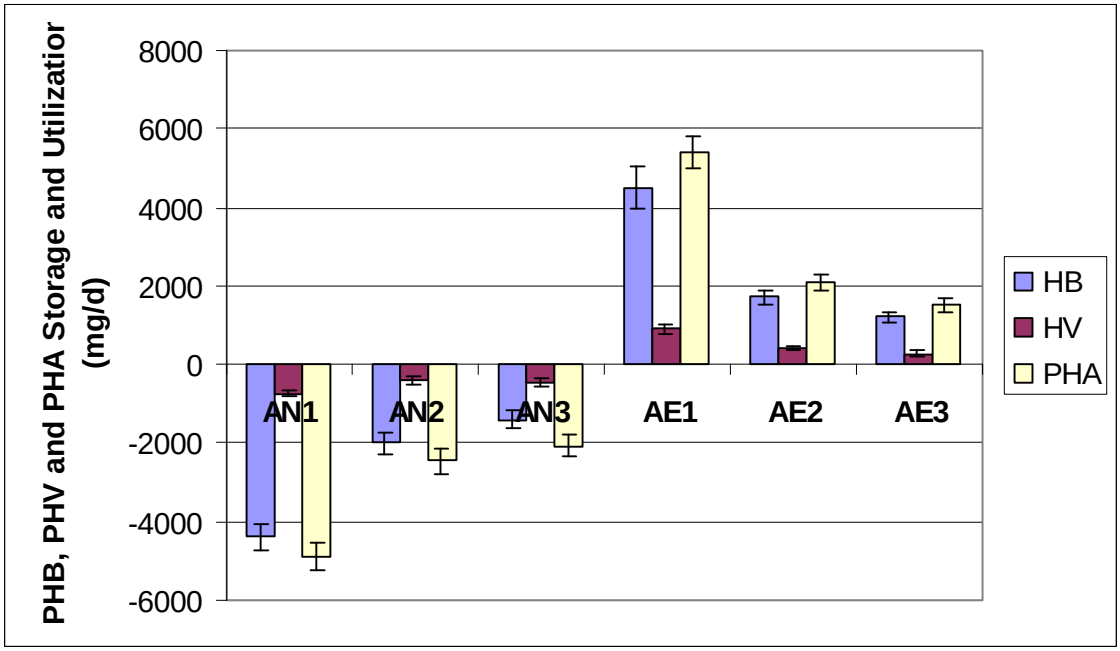

Figure 7. PHA storage and utilization pattern for the A/O system.

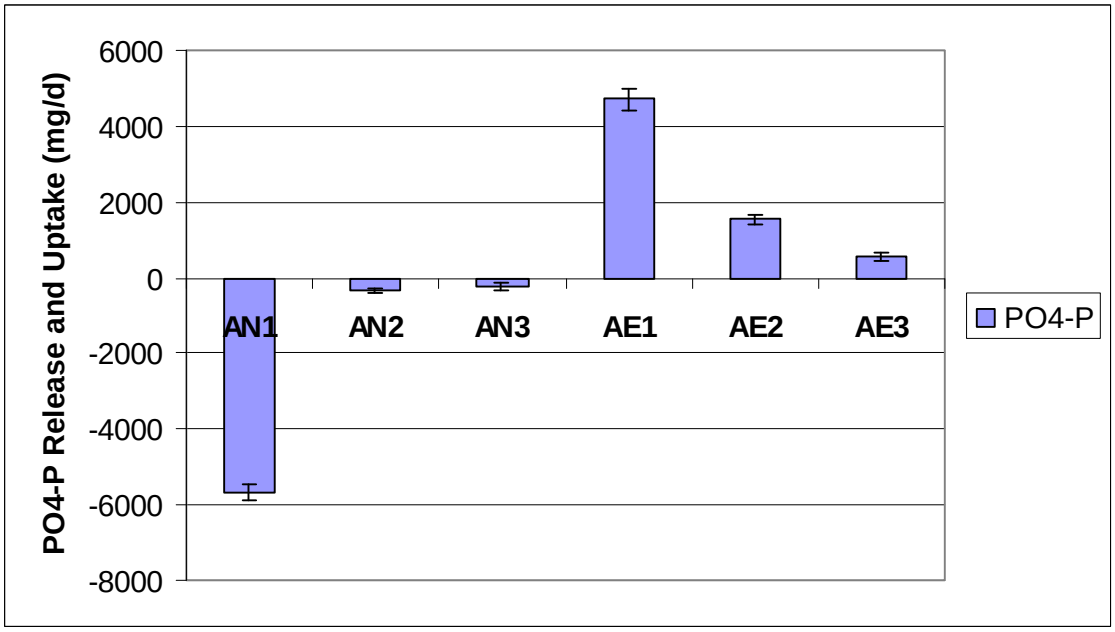

Figure 8. PO4-P release and uptake pattern for the A/O system.

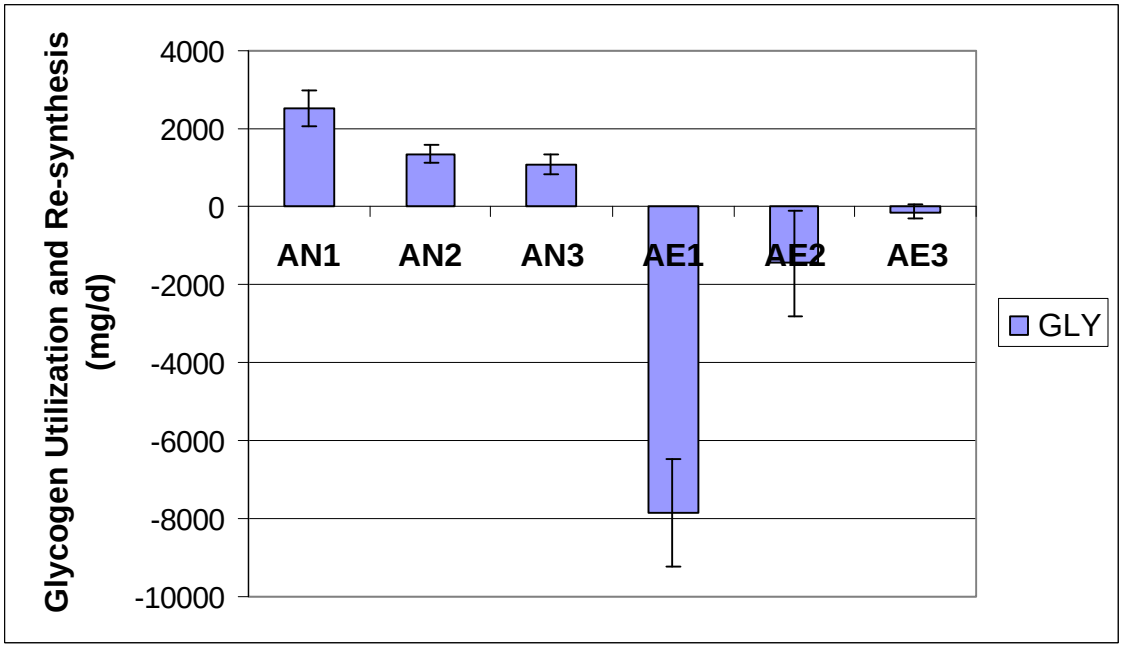

Figure 9. Glycogen consumption and re-synthesis pattern for the A/O system.

Table 2. Carbon and COD equivalents of acetate, PHB, PHV and glycogen

	Molecular formula	Monomer MW mg/mmol	Carbon mmolC/mg	COD mgCOD/mg
Acetate	CH_3COO^-	59	29.5	0.950
HB	$C_4H_6O_2$	86	21.5	1.674
HV	$C_5H_8O_2$	100	20	1.920
Glycogen	$C_6H_{10}O_5$	162	27	1.185

Table 3. Carbon and phosphorus balance for the A/O system.

Acetate$_{inf}$	C-mmol/d	366±6		Anaerobic Changes Per C-mmol of Acetate
PO4-P$_{inf}$	P-mmol/d	21±1.7		
		Anaerobic	Aerobic	
PO4-P	P-mmol/d	-201±12	220±16	0.55
HB	C-mmol/d	362±37	-346±39	0.99
HV	C-mmol/d	80±13	-79±14	0.22
PHA	C-mmol/d	442±50	-425±53	1.21
Glycogen	C-mmol/d	-183±34	349±108	0.50

The carbon and phosphorus balances for the A/O system (mmoles per day) calculated based on the conversion factors presented in Table 2 are given in Table 3. The conversions taking place under anaerobic conditions, i.e. uptake of acetate, storage of PHA, utilization of glycogen and release of phosphate, are in agreement with the correlation factors found in numerous studies as listed in Z. Erdal and Randall (2002a). As can be seen from Table 3, for 549 mmol/d available carbon in the anaerobic reactors, 442 mmol/d PHA carbon were produced. The difference can be attributed to the experimental limitations, or to the presence of other forms of storage products. Also partial loss of carbon in the form of CO_2 may be taking place. On the other hand, for 425 mmol/d PHA carbon utilized under aerobic conditions, 349 mmol/d glycogen carbon was stored, which to some extent implies that there is not a significant loss of organic carbon from the system, since there would be too few carbons left for new cell growth. To prevent CO_2 loss from the system, i.e. to conserve carbons and to increase the efficiency of storage reactions, more efficient biochemical pathways might be selected. Tables 4 through 7 give the mass balances for the internal storage products as measured in the UCT system under two different temperature conditions; 20° and 5°C.

Table 4. Average performance values for the UCT system at 20°C; value±S.E.M.

Inf COD mg/L	Inf PO4-P mg/L	Inf NH4-N mg/L
485±4.4	39±1.2	39±1.6

	AN1	AN2	AX1	AX2	AE1	AE2	AE3	EFF	RAS
PO4-P[1] mg/d	-4873±**106**	-2554 ± 126	299 ± 50	-499 ± 54	7152 ± 101	1380 ± 60	381 ± 66		
HB[2] mg/d	5421 ± 38	2781 ± 160	-255 ± 52	539 ± 68	-6015 ± 98	-1461 ± 136	-574 ± 110		
HV[2] mg/d	1190 ± 8	611 ± 34	-56 ± 12	118 ± 14	-1320 ± 22	-321 ± 30	-126 ± 24		
HA[2] mg/d	6612 ± 46	3392 ± 194	-310 ± 62	658 ± 82	-7335 ± 120	-1782 ± 164	-700 ± 134		
GLY[3] mg/d	-3728 ± 194	**-1645** ± 178	118 ± 56	-376 ± 50	4086 ± 276	1716 ± 194	363 ± 124		
OUR mg/L/hr					66 ± 1.9	31 ± 0.4	24 ± 0.5		
MLSS mg/L	2930 ± 34	2896 ± 34	4542 ± 26	4509 ± 44	4653 ± 56	4737 ± 56	4789 ± 42	36 ± 6	7578 ± 62
MLVSS mg/L	2112 ± 18	2107 ± 24	3246 ± 14	3238 ± 22	3255 ± 46	3303 ± 34	3280 ± 22	24 ± 4	5297 ± 30
%VSS	0.72 ± **0.01**	0.73 ± 0.01	0.71 ± 0.01	0.72 ± 0.01	0.70 ± 0.01	0.70 ± 0.01	0.68 ± 0.01	0.67±0.01	0.70±0.01

[1]Negative values indicate phosphate release, and positive values indicate phosphate uptake.

[2]Negative values indicate consumption, and positive values indicate storage.

[3]Negative values indicate glycogen utilization, and positive values indicate glycogen re-synthesis.

Table 5. Average performance values for the UCT system at 5°C; value±S.E.M.

Inf COD mg/L	Inf PO4-P mg/L	Inf NH4-N mg/L
499±7.4	147±9	33±1.6

	AN1	AN2	AX1	AX2	AE1	AE2	AE3	EFF	RAS
PO4-P[1] mg/d	-3008 ± 113	-1431 ± 64	-2465 ± 115	-1919 ± 88	6583 ± 257	3430 ± 151	2056 ± 277		
HB[2] mg/d	4371 ± 258	2311 ± 246	3448 ± 218	1873 ± 193	-5960 ± 336	-3251 ± 147	-1669 ± 129		
HV[2] mg/d	329 ± 19	174 ± 19	260 ± 16	141 ± 14	-449 ± 25	-245 ± 11	-126 ± 10		
HA[2] mg/d	4700 ± 277	2485 ± 265	3707 ± 234	2014 ± 207	-6408 ± 361	-3496 ± 158	-1795 ± 139		
GLY[3] mg/d	-1061 ± 126	**-696** ± 120	-1148 ± 176	-735 ± 86	2150 ± 314	1006 ± 119	590 ± 74		
OUR mg/L/hr					42 ± 2.9	32 ± 1.1	25 ± 1.1		
MLSS mg/L	4448 ± 141	4395 ± 146	7456 ± 255	7411 ± 240	7727 ± 230	7878 ± 243	7972 ± 247	44 ± 7	14350 ± 709
MLVSS mg/L	2779 ± 61	2781 ± 69	4518 ± 66	4543 ± 78	4557 ± 84	4537 ± 72	4506 ± 73	25 ± 4	8271 ± 205
%VSS	0.62 ± 0.01	0.63 ±0.01	0.61 ±0.01	0.61 ± 0.01	0.59 ±0.01	0.58 ±0	0.57±0.01	0.57±0	0.58 ±0.01

[1]Negative values indicate phosphate release, and positive values indicate phosphate uptake.

[2]Negative values indicate consumption, and positive values indicate storage.

[3]Negative values indicate glycogen utilization, and positive values indicate glycogen re-synthesis.

Table 6. Carbon and phosphorus balances for the UCT system at 20°C; value±S.E.M

Acetate$_{inf}$	C-mmol/d	517 ± 6		Non-oxic Changes Per C-mmol of Acetate
PO4-P$_{inf}$	P-mmol/d	43 ± 1.3		
		Non-oxic	Aerobic	
PO4-P	P-mmol/d	-246 ± 12	288 ± 7.4	0.48
HB	C-mmol/d	411 ± 2.4	-393 ± 2.6	0.80
HV	C-mmol/d	90 ± 1	-86 ± 0.6	0.17
PHA	C-mmol/d	501 ± 5.4	-479 ± 3.2	0.97
Glycogen	C-mmol/d	-211 ± 6.4	230 ± 8	0.41

Table 7. Carbon and phosphorus balances for the UCT system at 5°C; value±S.E.M

Acetate$_{inf}$	C-mmol/d	461 ± 8.2		Non-oxic Changes Per C-mmol of Acetate
PO4-P$_{inf}$	P-mmol/d	146 ± 8.9		
		Non-oxic	Aerobic	
PO4-P	P-mmol/d	-285 ± 6.7	389 ± 11	0.62
HB	C-mmol/d	562 ± 23	-510 ± 22	1.22
HV	C-mmol/d	42 ± 1.8	-38 ± 1.6	0.09
PHA	C-mmol/d	604 ± 25	-548 ± 23	1.31
Glycogen	C-mmol/d	-135 ± 11	139 ± 14	0.29

The calculated mass balance values indicate that there was a shift in the distribution of the storage products as the UCT system acclimated to the temperature stress because an increase in net PHA production and a decrease in glycogen utilization was observed. Also, a decrease in concomitant glycogen storage in the aerobic reactors was observed. This can either be attributed to possible population shifts or to shifts in active microbial metabolism. The differentiation of these two factors may not be very easy, as either one may be mistaken for the other. During a population shift, the changes that take place in microbial group identities may pose themselves like metabolism shifts. Hence, to distinguish between the two, U. Erdal (2002) performed electron microscopic analyses of biomasses that were cultivated under the same feed and operating conditions but different temperatures. They have shown that at 20°C, the biomass contained a much more diverse group of organisms whereas at 5°C the diversity was replaced with a dominating group of organisms able to store very large vacuoles full of poly-P. Hence the change in storage pattern was mainly due to a switch from one type of microbial community to another. To explain the underlying mechanisms causing the observed differences in culture response between the two biomasses, the results of the enzyme study and NMR study will be reviewed.

Glycogen Metabolism Inhibition Experiments

Six potential inhibitors of glycogen metabolism were tested. Results of the inhibitor screening experiments performed on the aerobic A/O biomass, i.e., biomass loaded with stored poly-P and glycogen, in a series of batch tests are given in Table 8. Deoxyglucose, DTNB, and deoxynojirimycin had no apparent effect on the EBPR functions. At 0.15 M initial concentration, 3-Ortho-methyl glucose did cause an increase in phosphate release that was not accompanied with an increased phosphate uptake. Moreover, glycogen consumption increased while the PHA storage was less than half of the control value. Thus it caused an imbalance in the microbial activity. Reduced glutathione caused a similar impact on the EBPR metabolism.

Table 8. Results of the inhibitor screening study completed as a series of batch tests performed on A/O sludge

Inhibitor	Init C M	Init Ac mg/L	MLSS mg/L	Anaerobic PO4-P release mg/L	Aerobic PO4-P uptake[1] mg/L	Anaerobic Glycogen Utilization mg/L	Aerobic Glycogen Synthesis[2] mg/L	Anaerobic PHA Synthesis mg/L	Aerobic PHA Consumption[3] mg/L
Deoxyglucose	0.029	254	1275	40	18	52	-3		
DTNB	0.25	254	1275	40	19	44	-16		
Control	0	254	1275	40	25	54	4		
Deoxynojirimycin	0.105	346	1300	97	65	64	18		
DTNB	0.35	346	1300	81	38	59	8		
Control	0	346	1300	86	58	62	38		
Gluconolactone	0.05	260	1156	63	43	64		211	180
Gluconolactone	0.2	260	1156	60	21	57	27		
Gluconolactone	0.43	108	1341	22	-28	61	-5		
Gluconolactone	0.46	130	1167	19	-6.5	57	-0.1	35	-15
Gluconolactone	0.46	260	1156	20	-37	37	-29	95	49
Control	0	108	1156	69	79	58	34		
Control	0	130	1156	66	71	78	61	69	59
Control	0	260	1156	58	65	101	171	252	238
3-ortho-methyl glucose	0.05	181	1207	72	20	40	35	8.5	5.1
3-ortho-methyl glucose	0.15	181	1207	96	19	72	30	12	1.8
Control	0	181	1207	74	84	39	68	27	26
Glutathione (red.)	0.01	181	1207	75	22	52	36	17	7
Glutathione (red.)	0.02	181	1207	84	5	52	31	13	6
Control	0	181	1207	74	84	39	68	27	26

[1]Negative values indicate phosphate release.

[2]Negative values indicate glycogen utilization.

[3]Negative value indicates PHA storage.

The greatest impact was caused by gluconolactone, which was tested several more times than the others. In each case anaerobic P-release was much less then that of the control and the subsequent aerobic P-uptake was also much less then that of the control. Especially when the initial gluconolactone concentration was increased above 0.40 M, the P-release continued during the aerobic period, and was accompanied by aerobic glycogen utilization. Although there was an overall decreasing trend, PHA response was sporadic. Figures 10 through 13 illustrate the observed responses from the EBPR sludge to varying initial concentrations of gluconolactone. Keeping in mind that gluconolactone was selected from possible glycogen phosphorylase inhibitors, Figure 10 casts doubt on the presence of such an inhibition, at least in this study where the inhibitor was not applied directly to cell extracts or to purified enzyme. In Figure 10, if the low point (37 mg/L) is not considered the regression line would be even flatter, more strongly implying the absence of an inhibition of glycogen phosphorylase. The actual impact must be on other enzymes, since the phosphate release (Figure 11) and uptake (Figure 12) were adversely and linearly affected by gluconolactone. The strong decreasing trend observed in Figure 13 may be because of the decreased anaerobic PHA production, which led to lower consumption in the following aerobic period. Thus, these results have shown that even gluconolactone, which seemingly resulted in inhibited EBPR behavior, was not a reliable inhibitor of glycogen phosphorylase for this study. Another deficit of gluconolactone was that it required extremely high dosages to be inhibitory. A calculation of the required concentration for a continuous system revealed that, for 50 L daily feed preparation, to achieve 80 g/L (0.46 M) in the initial reactors, at least 8 kg of gluconolactone was necessary. Therefore, this unrealistic pursuit was abandoned, especially considering that cold temperature was found to suppress glycogen metabolism much more reliably.

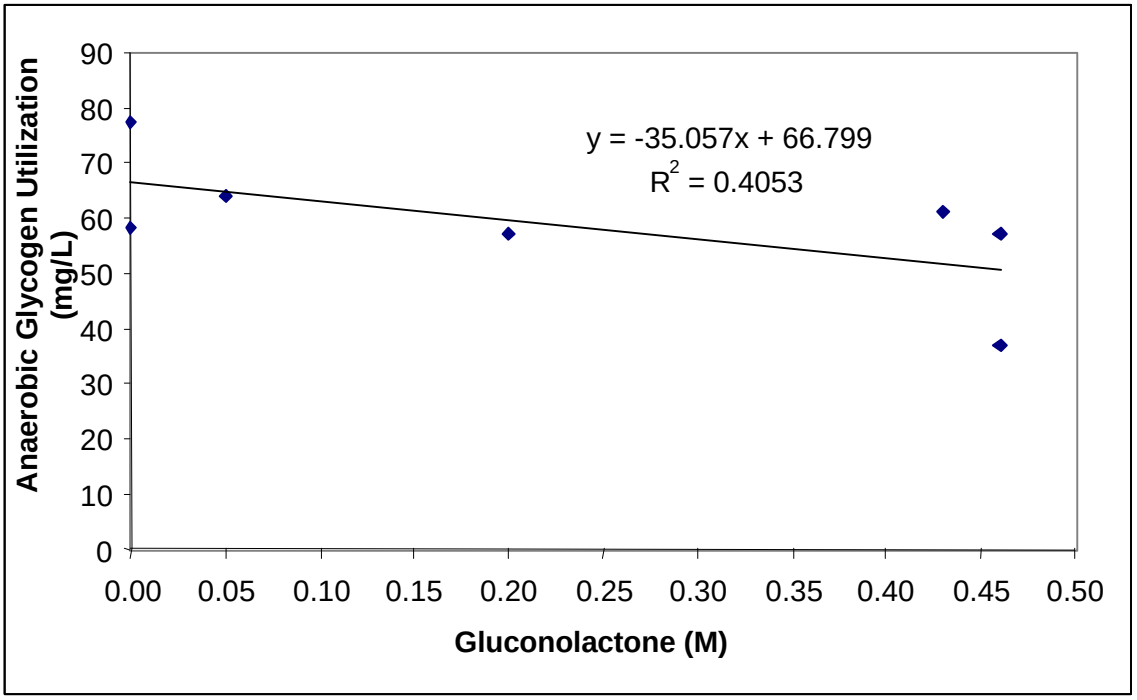

Figure 10. The response of anaerobic glycogen metabolism to varying concentrations of gluconolactone.

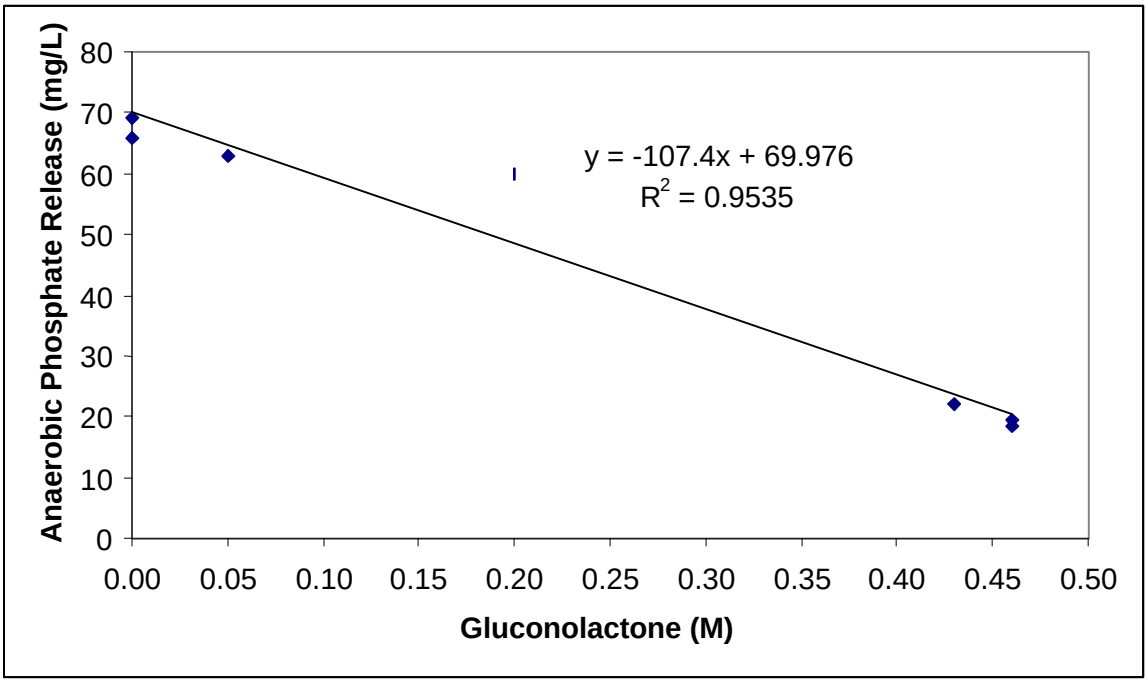

Figure 11. The response of anaerobic phosphate metabolism to varying concentrations of gluconolactone.

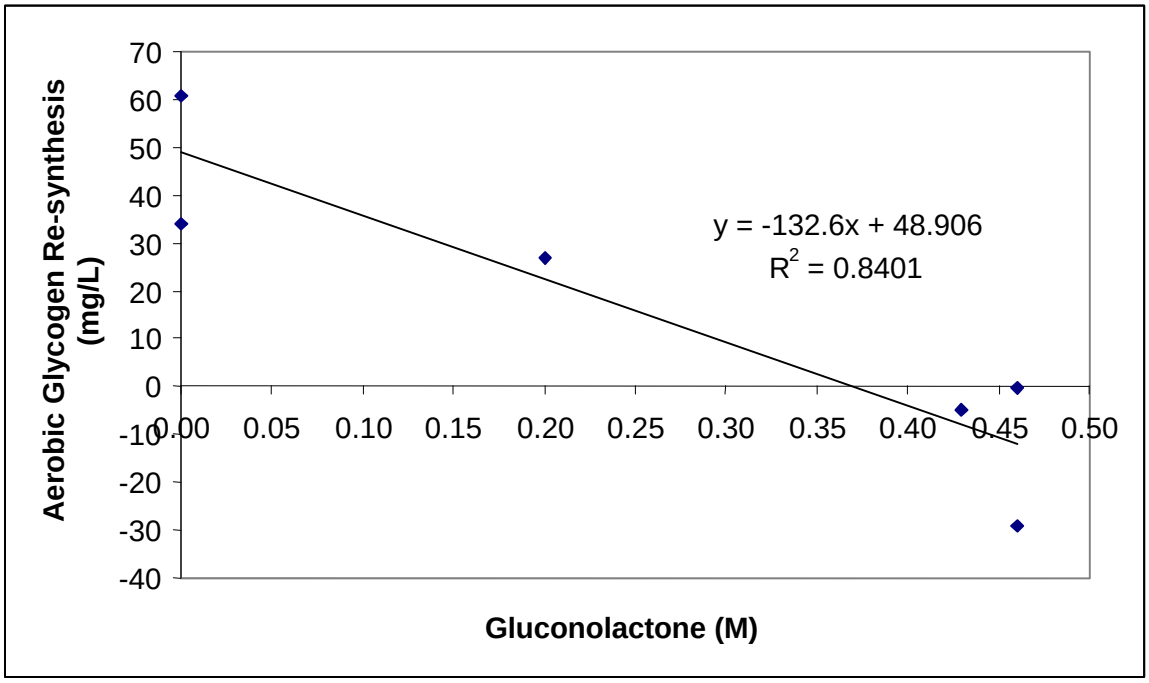

Figure 12. The response of aerobic glycogen metabolism to varying concentrations of gluconolactone.

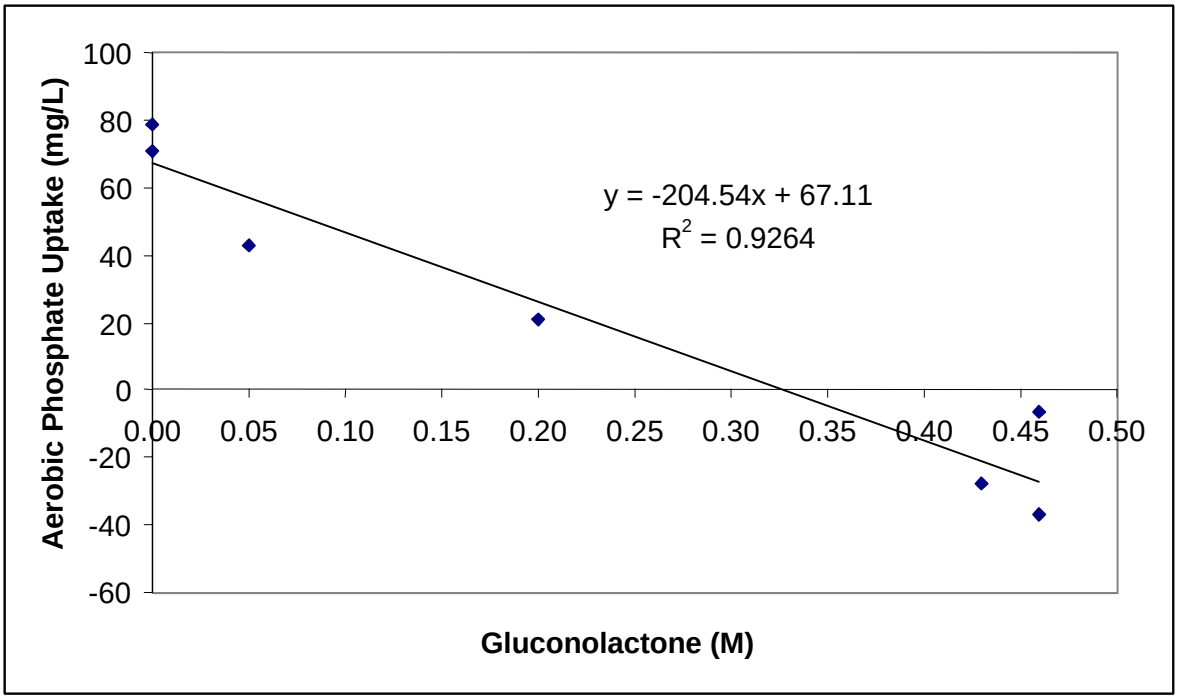

Figure 13. The response of aerobic phosphate metabolism to varying concentrations of gluconolactone.

Active Enzyme Systems of the EBPR Metabolism

Enzyme assays performed on the EBPR biomass obtained from the 20° and 5°C sludges yielded very useful results. A summary of the enzymes that were included in this study, the pathways in which they are involved, and the results of the enzyme assays are summarized in Table 9. As explained earlier, the enzymes were selected such that the presence or absence of their activity would indicate the presence or the absence of the specific pathway in which the enzymes take part. In other words, the enzymes selected were considered to be "key enzymes" of the individual pathways. The results showed that many of the chosen enzymes were active under both anaerobic and aerobic conditions under both temperature conditions, with the exception of fumarate reductase. It is important to emphasize that some of this activity can be residual activity. What the UCT configuration imposes on the EBPR biomass is that it is sequentially recycled between reactors where the electron acceptors are absent in one and available in the other. That is to say the biomass is recycled between the anaerobic reactors where the VFAs are available, but electron acceptors are absent, and the aerobic reactors where the VFAs are all taken up, but electron acceptors are available. Thus, the enzyme machinery can be acclimated to the recycling between the absence and presence of terminal electron acceptors, and it may be adjusted so that enzyme activity will be retained in order to save energy by not having to re-synthesize the enzymes each time the conditions change. However, this in turn brings about the question of which enzyme is actually active and which enzyme is purposefully present. To determine this, NMR analysis was performed to supplement the information available.

The results of the enzyme activity assays are presented in Table 10. Isocitrate dehydrogenase, which catalyzes oxidative decarboxylation of isocitrate to α-ketoglutarate, producing one NADH and one CO_2, is a part of the TCA cycle. The specific activities of the enzymes present in the 20° and 5°C activated sludge samples indicated a higher activity for the latter group of samples, especially in the aerobic reactors (Table 11). Malate dehydrogenase, another TCA cycle enzyme responsible for the oxidation of malate or reduction oxaloacetate, i.e. the forward and reverse reactions

between malate and oxaloacetate, showed high specific activity in all cases. The anaerobic activity of the enzyme was higher than the aerobic activity in all cases but one; the September 17 sample.

Table 9. Enzyme assays performed on EBPR biomass samples taken during operation of the UCT system. (+ : present; - : absent)

Enzymes	Malate Synthase		Isocitrate Lyase		Malate DH		Isocitrate DH		Fumarate Reductase		α-KG DH*		PFK		G6P DH		Methylmalonyl Mutase		Methylmalonyl decarb	
Pathways in which the enzymes are involved	Glyoxylate Shunt		Glyoxylate Shunt		Glyoxylate Shunt								EMP Pathway		PP Pathway		SuccCoA->MMCoA		MMCoA->PropCoA	
					TCA Cycle		TCA Cycle				TCA Cycle				ED Pathway					
					Branched TCA		Branched TCA		Branched TCA											
					Reverse (Red.) TCA		Reverse (Red.) TCA		Reverse (Red.) TCA											
					Succ.-Prop. Pathway				Succ.-Prop. Pathway											
	An/Ae	An/Ae	An/Ae	An/Ae	An/Ae	An/Ae	An/Ae	An/Ae	An	An	An/Ae	An/Ae	An/Ae	An/Ae	An/Ae	An/Ae	An/Ae	An/Ae	An/Ae	An/Ae
Sample	20C	5C	20C	5C	20C	5C	20C	5C	20C	5C	20C	5C	20C	5C	20C	5C	20C	5C	20C	5C
28-Jun	+	+	-	-	+	+	+	+	+	-	-	-	+	+	-	-	+	+	+	+
17-Sep	+	+	-	-	+	+	+	+	+	-	-	-	+	+	-	-	+	+	+	+
19-Oct	+	+	-	-	+	+	+	+	+	-	-	-	+	+	-	-	+	+	+	+

*Activity of α-KG DH enzyme complex was probably lost during sample preparation

Table 10. The results of the enzyme activity assays.

Temp.	Date	Reactor	Protein μg/mL	Sp.Activity U/mg
Isocitrate Dehydrogenase				
E=15mM-1cm-1				
20°C	10/19	AN	1.91	0.0014
		AE	3.99	0.0024
5°C	10/19	AN	2.26	0.0142
		AE	8.65	0.0361
20°C	9/17	AN	2.96	0.0008
		AE	1.72	0.0014
5°C	9/17	AN	2.6	0.0123
		AE	1.86	0.0323
20°C	6/28	AN	1.24	0.0009
		AE	1.78	0.0012
5°C	6/28	AN	0.97	0.0134
		AE	1.12	0.0297
PFK				
E=6.22 mM-1 cm-1				
20°C	10/19	AN	1.91	0.0925
		AE	3.99	0.0581
5°C	10/19	AN	2.26	0.0684
		AE	8.65	0.0408
20°C	9/17	AN	2.96	0.1939
		AE	1.72	0.1733
5°C	9/17	AN	2.6	0.0722
		AE	1.86	0.0534
20°C	6/28	AN	1.24	0.0874
		AE	1.78	0.0542
5°C	6/28	AN	0.97	0.0622
		AE	1.12	0.0487
Malate Dehydrogenase				
E=15mM-1cm-1				
20°C	10/19	AN	1.91	1.0995
		AE	3.99	0.6015
5°C	10/19	AN	2.26	0.5752
		AE	8.65	0.1734
20°C	9/17	AN	2.96	0.6419
		AE	1.72	0.7267
5°C	9/17	AN	2.6	0.2115
		AE	1.86	0.3495
20°C	6/28	AN	1.24	0.7416
		AE	1.78	0.4473
5°C	6/28	AN	0.97	0.3478
		AE	1.12	0.1059

Temp.	Date	Reactor	Protein μg/mL	Sp.Activity U/mg
Fumarate Reductase				
E=0.78 mM-1cm-1				
20°C	10/19	AN	1.91	0.1579
		AE	3.99	No assay
5°C	10/19	AN	2.26	0
		AE	8.65	No assay
20°C	9/17	AN	2.96	0.1674
		AE	1.72	No assay
5°C	9/17	AN	2.6	0
		AE	1.86	No assay
20°C	6/28	AN	1.24	0.1349
		AE	1.78	No assay
5°C	6/28	AN	0.97	0
		AE	1.12	No assay
Malate Synthase				
E=13.6 mM-1 cm-1				
20°C	10/19	AN	1.91	0.0037
		AE	3.99	0.1278
5°C	10/19	AN	2.26	0.0763
		AE	8.65	0.1451
20°C	9/17	AN	2.96	0.0238
		AE	1.72	0.2964
5°C	9/17	AN	2.6	0.1207
		AE	1.86	0.3795
20°C	6/28	AN	1.24	0.0027
		AE	1.78	0.1076
5°C	6/28	AN	0.97	0.0914
		AE	1.12	0.2491

Since the G°' of the malate dehydrogenase reaction is +29.7 $kJ \cdot mol^{-1}$, oxaloacetate formation requires conditions that favor the reaction (Voet and Voet, 1995). One of these conditions can be that there needs to be a high enough concentration of malate and malate dehydrogenase for the reaction to produce just a small quantity of oxaloacetate. The G°' of the citrate synthase is low enough (-31.5 $kJ \cdot mol^{-1}$) to drive the reaction even when there is a small amount of oxaloacetate present, and the cycle can keep running even at low concentrations of oxaloacetate. This may be one reason why the specific activity values of malate dehydrogenase were measured to be the highest activity values among all the examined enzymes. The values of the anaerobic versus aerobic specific activities of malate dehydrogenase were very close, and the presence of this enzyme can indicate the operation of one or more of these pathways: TCA cycle, glyoxylate shunt, or branched TCA cycle.

Fumarate reductase of the branched TCA cycle gave one of the key clues to what kind of metabolism was used under anaerobic conditions at 20° and 5°C by biomass samples. It was found that the enzyme, which replaces succinate dehydrogenase of the TCA cycle and catalyzes the reaction from fumarate to succinate and consumes one $FADH_2$, was absent in all 5°C samples. This clearly indicates that there is a significant metabolic difference between the two biomasses. This result combined with the specific activity pattern detected for malate synthase of the glyoxylate shunt indicates that under cold temperature conditions, the glyoxylate shunt was favored over the branched TCA pathway for anaerobic activity. Although aerobic samples showed higher activity of malate synthase for all cases, at cold temperatures the differences between the aerobic and anaerobic sample activities were smaller (Table 11). Thus, the glyoxylate shunt appears to be the preferred anaerobic route for the cold cultivated culture. In the aerobic zone use of the glyoxylate shunt allowed the cells to metabolize acetate to C4 intermediates (oxaloacetate and malate) that could be used to re-synthesize glycogen. Moreover, oxaloacetate is precursor for aspartate and asparagine required for protein biosynthesis.

Table 11. Comparison of the anaerobic and aerobic activities of the investigated enzymes

Temp.	Date	Sp.Activity Anaerobic/Aerobic	Temp	Date	Sp.Activity Anaerobic/Aerobic
Isocitrate Dehydrogenase			*Fumarate Reductase*		
20°C	10/19	0.59	20°C	10/19	N/A
5°C	10/19	0.39	5°C	10/19	N/A
20°C	9/17	0.58	20°C	9/17	N/A
5°C	9/17	0.38	5°C	9/17	N/A
20°C	6/28	0.75	20°C	6/28	N/A
5°C	6/28	0.45	5°C	6/28	N/A
PFK			*Malate Synthase*		
20°C	10/19	1.59	20°C	10/19	0.03
5°C	10/19	1.67	5°C	10/19	0.53
20°C	9/17	1.12	20°C	9/17	0.08
5°C	9/17	1.35	5°C	9/17	0.32
20°C	6/28	1.61	20°C	6/28	0.03
5°C	6/28	1.28	5°C	6/28	0.37
Malate Dehydrogenase					
20°C	10/19	1.83			
5°C	10/19	3.32			
20°C	9/17	0.88			
5°C	9/17	0.61			
20°C	6/28	1.66			
5°C	6/28	3.28			

N/A: not applicable

One other enzyme that was clearly active under all conditions was the phosphofructokinase (PFK) enzyme of the EMP pathway, and it catalyzes the phosphorylation of fructose-6-P to fructose-1,6-bisphosphate, at the expense of one ATP. The fact that PFK showed positive activity, and that the activity of glucose-6-P dehydrogenase of the ED and pentose phosphate pathways was absent, clearly indicates that glycolysis proceeds via the EMP pathway instead of the ED and PP pathways. This fact does not make any difference in the amount of the final product (pyruvate) of the glycolysis, but it changes the numbers of ATP and NADH produced per glucose released from the glycogen chain via glycogen phosphorylase reaction. Thus, the suggestion of Wentzel *et al*. (1991) that the ED pathway not the EMP must be operative because of the absence of the latter one in *Acinetobacter* spp. cannot be true.

Two final enzymes examined were methylmalonyl-CoA mutase and methylmalonyl-CoA decarboxylase which catalyze the conversions of succinyl-CoA to methylmalonyl-CoA and then to propionyl-CoA, respectively, under anaerobic conditions, which eventually ends up as the fifth carbon of the hyroxyvaleryl units of the PHA polymer. The enzymes reverse these reactions under aerobic conditions. Because a properly defined activity measurement method other than that given in Bermudez *et al*. (1998) was not available for these enzymes, and the method presented in Bermudez *et al*. (1998) was incomplete, the HPLC measurements did not yield quantitative data. The best values for eluent flow rates, and for eluent A and eluent B combination (97 to 3 percent) was determined by trial and error. Besides, due to the interference of the enzyme assay matrix, a reliable standard curve could not be generated. However, the disappearance of the enzyme substrate and generation of the product were apparent. Thus, it was concluded that both of these enzymes were active under all conditions, and all the crude extract samples resulted in similar levels of activity in terms of product formation, although exact values for the activity could not be determined.

Solid State NMR Analysis of the EBPR metabolism at 20^{o}C

Table 12 and Table 13 present the results of the NMR experiments. The chemical shifts that correspond to the PHA carbons are C-1 at 170 ppm, C-2 at 40 ppm, C-3 at 68 ppm, C-4 at 22 ppm, and C-5 at 10 ppm. Similarly, the chemical shifts that correspond to the glycogen carbons are C-1 at 100 ppm, C-2 to 5 between 70 and 73 ppm, and C-6 at 62 ppm. Thus, at the end of the first anaerobic period, the label on the first carbon of acetyl-CoA ended up on the first and third carbons of the PHA units, and no label on the fifth carbon was observed, at both temperatures. During the first aerobic period, the label remaining from the breakdown and oxidation of PHA units was distributed between C-2 to 5 of glycogen and carboxyl units of PHA and possibly other newly formed cell components. When the remaining label was subjected to a second anaerobic period, label at C-4 of PHA was detected. Remaining label was left on the unused glycogen and the carboxyl groups as mentioned before. Finally, when the end of the second aerobic period was reached, the labels were transferred back on the glycogen (C2-5) and on the carboxyl carbons.

The label transfer for the acetyl-CoA that was labeled at the second carbon, on the other hand, was also very consistent with the known acetoacetate formation from two acetate units: the label was at the second and the fourth carbon. Interestingly, the label was not distributed evenly between the second and fourth carbons, and C-4 received more label (65%) compared to C-2 (35%). Following the aerobic period, the label distribution indicated formation of glycogen with 50% of the label being transferred to C2-6 of glycogen, while the first carbon received 14% of the remaining label. At the end of the second anaerobic period, the label that remained in the system was transferred to C-4 of PHA, while the C-1 of glycogen disappeared. During the next aerobic period the label in the PHA units were transferred back to the newly synthesized glycogen molecules (53 % to C2-6, 10% to C1). The remaining label at the end of the second aerobic period was enough to yield significantly sharp peaks, indicating that fewer carbons were lost as CO_2 as would be expected.

Table 12. Distribution of the labeled carbon (C_0=4.75mM) between different points on the intracellular storage products at 20°C.

20C	time	C-1 label relative peak area (%)			
	hr	22ppm	68ppm	73ppm	170ppm
Anaerobic	0		68		42
	2		49		51
Aerobic	4			66	34
	6			65	35
Anaerobic	0			62	38
	2	12		43	38
Aerobic	4			60	40
	6			69	31

	Time	C-2 label relative peak area (%)					
	hr	22ppm	42ppm	62ppm	73ppm	102ppm	172ppm
Anaerobic	0						
	2	65	35				
Aerobic	4	20		18	36	16	10
	6	22		52		14	10
Anaerobic	0						
	2	43		40			17
Aerobic	4	24		16	41	9	11
	6	22		53		10	15

Table 13. Distribution of the labeled carbon (C_0=6.0mM) between different points on the intracellular storage products at 5°C.

5C	Time	C-1 label relative peak area			
	Hr	22ppm	68ppm	73ppm	170ppm
Anaerobic	0				
	3.5		53		47
	7		52		48
Aerobic	9		51		49
	13		17	45	38
	24		16	47	37
Anaerobic	0			57	43
	9.5		40		60
Aerobic	24		40		60

	Time	C-2 label relative peak area							
	Hr	10ppm	22ppm	42ppm	62ppm	68ppm	73ppm	102ppm	172ppm
Anaerobic	0								
	3.5		55	45					
	7		54	46					
Aerobic	9		23	14	17		30	16	
	13		19	12	19		33	18	
	24		14	11	24		31	20	
Anaerobic	0								
	9.5	8	35	23		21			13
Aerobic	24	5	37	25		33			16

Solid State NMR Analysis of the EBPR Metabolism at 5^{o}C

A similar carbon labeling study was performed at 5°C and the following labeling patterns were observed: The acetate labeled at the first carbon resulted in the formation of PHA labeled equally at the first and the third carbons (48% and 52%, respectively), very similar to what was observed at 20°C. The first aerobic period gave rise to the synthesis of glycogen labeled at C2-5, while a significant amount of label remaining on PHA C-3 and C-1. Most of the label transferred to glycogen came from the C-3 of the PHA units. By the end of the aerobic period, most of the label was lost, as indicated by the difference in the intensity of the peaks (Appendix B). When the sludge was exposed to a second anaerobic period, there was not much label left to go around, and most of it was stored in carboxyl groups (170ppm). Thus, the second cycle of anaerobic-aerobic exposure was not very instructive.

The acetate labeled at the second carbon resulted in the formation of PHA labeled reasonably equally at the second and the fourth carbons (46% and 54%, respectively), which was different from what was observed at 20°C. At the end of the aerobic period, the labels on the PHA were partially distributed to the glycogen (C-1 20%, C2-5 31%, and C-6 24%). When the sludge was exposed to another anaerobic-aerobic cycle, all the label on the glycogen were transferred back to the newly synthesized PHA units, also resulting in labeling at C-5 of hydroxyvalerate at 10 ppm. During the last aerobic period a peculiar result was observed. No glycogen formation (no peaks at 62, 73 or 102 ppm) was detected, and the peak intensities remained almost unchanged. PHA synthesized from the non-labeled acetate introduced at the beginning of the second anaerobic-aerobic cycle must be utilized during the second aerobic period, somehow leaving the labeled PHA units unused.

Combining the results obtained so far, a biochemical picture of the carbon transformations taking place in the anaerobic and aerobic reactors of the EBPR systems can be drawn using the results obtained with the 20°C and 5°C activated sludges. Considering the active pathways determined during the enzyme activity study, a theoretical label tracking analysis of the possible pathways was performed. Thus, knowing that the only source of label during the first anaerobic stage was the feed acetate labeled at the first and second carbon, it is straightforward to determine that the labels will be transferred to the 1st and 3rd carbon of PHB for C*-1 labeled acetate, and to the 2nd and 4th carbon of the newly synthesized PHB for C*-2 labeled acetate, through condensation of two acetyl-CoA units into one acetoacetyl-CoA, and then its polymerization into hydroxybutyrate units. Since no peaks were detected to indicate the presence of labeled carbon at the 5th carbon of the hydroxyvalerate units, such a label transfer was also disallowed during the theoretical analysis. To analyze the possible contribution of the non-labeled glycogen degradation during the first anaerobic stage for the 20°C sludge, non-labeled pyruvate (from glycogen) and labeled acetate (from the feed) were considered to have entered the branched TCA cycle, since malate dehydrogenase and fumarate reductase activities were found to be positive. Succinyl-CoA formed from oxaloacetate (from pyruvate) would not receive any label if the glyoxylate shunt was inactive, in spite of the positive activity of enzyme malate synthase. Then, the source of the label transferred to succinyl-CoA would be the labeled acetyl-CoA that condenses with the non-labeled oxaloacetate. From there the label from C*-1 acetate would be released as CO_2, and label from C*-2 acetate would show up at the 4th carbon of the PHA units, which may explain the excess label detected at the C-4 position for C*-2 run (Table 12).

During the first aerobic stage the labeled PHA units will be degraded into acetyl-CoA units labeled at either C-1 or C-2 positions. When these acetyl-CoA units were assumed to go through the TCA cycle and the glyoxylate shunt, it was found that oxaloacetate that will be used for gluconeogenesis of new glycogen could be labeled in two ways. For the case of the TCA cycle, the label on the 4th carbon would be from C*-2 acetate, and for the case of the glyoxylate shunt, the source of the label would be C*-1 acetate. However,

the fourth carbon is released during the conversion of oxaloacetate to phosphoenolpyruvate, and the resultant glycogen formed from both cases contains a similar labeling pattern: labels on 3rd and 4th carbons from C*-1 acetate, labels on 1st, 2nd, 5th, and 6th carbons from C*-2 acetate.

When the second anaerobic-aerobic cycle starts, the sludges were allowed to settle and the supernatant was replaced with an equal volume of nutrient solution containing non-labeled acetate. Thus, at the end of the second anaerobic period the only source of label was the pyruvate generated from labeled glycogen breakdown. When this labeled pyruvate, some labeled acetyl-CoA that may be forming from labeled pyruvate, and non-labeled acetyl-CoA enter the branched TCA cycle, the resultant succinyl-CoA would contain C*-1 label on C-1, and C*-2 label on C-2 and C-3. Succinyl-CoA produced from the citrate side of the branch would contain C*-2 labels on all of its carbons. Thus, the resultant hydroxybutyrate and hydroxyvalerate units would contain only C*-2 label which would be at C-1,2,4,5. Table 11 shows that all of these were detected, except C-2 (40 ppm). This was because the peak was not very big and the interference from adamantane made it difficult to make a reasonably accurate relative peak area reading. Coming to the second aerobic stage, the source of label was acetyl-CoA (mostly non-labeled, some labeled at C-1,2 from C*-2) and propionyl-CoA (labeled at units released from the breakdown of the PHA units. Oxaloacetate formed from these would be labeled from C*-2 at all carbons, yielding glucose units labeled at all carbons. C*-1 carbons would either release as CO_2 or be left over in the unused glycogen and PHA remaining from the end of the first anaerobic-aerobic cycle. Consistent with the peak intensities, C*-2 carbons would be constantly transferred between carbon storage materials, and certainly some transferred to anabolic intermediates. However, their loss as CO_2 would be minimal.

When a similar analysis on the results of the 5°C NMR experiment was performed some differences were observed. Again, knowing that the only source of label during the first anaerobic stage was the feed acetate labeled at the first and second carbon, it was determined that the labels would be transferred to the 1st and 3rd carbon of PHB for C*-1

labeled acetate, and to the 2nd and 4th carbon of the newly synthesized PHB for C*-2 labeled acetate, through condensation of two acetyl-CoA units into one acetoacetyl-CoA, and then its polymerization into hydroxybutyrate units. Although compared to the earlier NMR study, more label was utilized to be able to detect small peaks, no peak at 10ppm was detected to indicate the presence of label at the 5th carbon of hydroxyvalerate units. Non-labeled glycogen degradation during the first anaerobic stage for the 5°C sludge, non-labeled pyruvate (from glycogen) and labeled acetate (from the feed) were considered to enter the glyoxylate shunt, since fumarate reductase activity was found to be negative at 5°C, and malate synthase activity was present and higher then what it was for 20°C. It is known that succinyl-CoA formed from lysis of isocitrate receives label when the glyoxylate shunt operates. Label is also transferred to succinyl-CoA during the condensation of the labeled acetyl-CoA and glyoxylate. After three turns of the cycle, some of the succinyl-CoA will be labeled at all carbons (C*-1 at C-1,4 and C*-2 at C-2,3). When the aerobic stage is started, the labels on acetyl-CoA originating from the breakdown of the PHA units will be transferred to oxaloacetate in the TCA cycle, which results in significant loss of labeled carbons (2 lost per turn). The labeling pattern on the newly synthesized glycogen (Table 12) would be the same as that at 20°C: labels on 3rd and 4th carbons from C*-1 acetate, labels on 1st, 2nd, 5th, and 6th carbons from C*-2 acetate. In the following second anaerobic cycle, label released from glycogen breakdown would be on pyruvate (C*-1 at C-1; C*-2 at C-2,3) and after three turns of the cycle all the carbons on succinyl-CoA would be labeled from C*-2, except C-1 that gets its label from C*-1. This explains the HV units labeled at C-5 with C*-2 carbons, and the reappearance of C-3 of PHA (68ppm) labeled with C*-1. Although C*-1 carbons are almost completely removed from the system at this point, C*-2 carbons are successfully conserved. Due to the generation of malate through action of two different enzymes (malate synthase – from glyoxylate/acetyl-CoA condensation, and fumarase - from succinate formation), there must be label on C-3 of PHA units that is of C*-2 origin. This fits the C*-2 NMR data which shows a peak at 68ppm (C-3) as well as on the remaining carbons of the HB/HV copolymer. After this point the NMR data did not show much change in the label distribution.

Proposed Biochemical Routes for EBPR Metabolism

In the light of the foregoing interpretation of the NMR data and theoretical label tracking through possibly operating pathways, the following metabolism is suggested for the EBPR biomasses studied, which were significantly enriched with poly-P removing organisms under acetate feed:

Based on enzymatic data, it is proposed that at both temperatures, anaerobic metabolism of the EBPR sludge included the EMP pathway following the phospholysis of glucose units from glycogen, as illustrated in Figure 14. At 20°C the carbons follow through to the branched TCA cycle (Figure 15) while the HB and HV units of the PHA copolymer are also produced. The aerobic metabolism, on the other hand, is proposed to go through the glyoxylate cycle while PHA breakdown provides the acetyl-CoA necessary to operate the cycle. Propionyl-CoA released from the HV units are converted to pyruvate (Voet and Voet, 1995) before they can partition between the glyoxylate cycle (Figure 16) and gluconeogenesis, which would operate in the reverse direction of what is shown in Figure 14, starting from oxaloacetate generated in the glyoxylate cycle. The only difference would be that phosphofructokinase is a unidirectional enzyme and for this reason Fructose-1,6-bisphosphatase is active during gluconeogenesis. Generation of glycogen after glucose-1-P is generated is accomplished by glycogen synthase.

At 5°C, on the other hand, anaerobic metabolism is proposed to proceed through the glyoxylate cycle based on the fact that fumarate reductase was not found in the 5°C biomass samples (Figure 17). The specific activity of the succinate dehydrogenase, and the relative activities of succinate dehydrogenase and succinyl-CoA synthatase will determine the distribution of succinate between fumarate and succinyl-CoA. The aerobic metabolism including the oxidation of PHA via TCA cycle (Figure 18) is also proposed and the glycogen synthesis also proceeds via gluconeogenesis similar to 20°C.

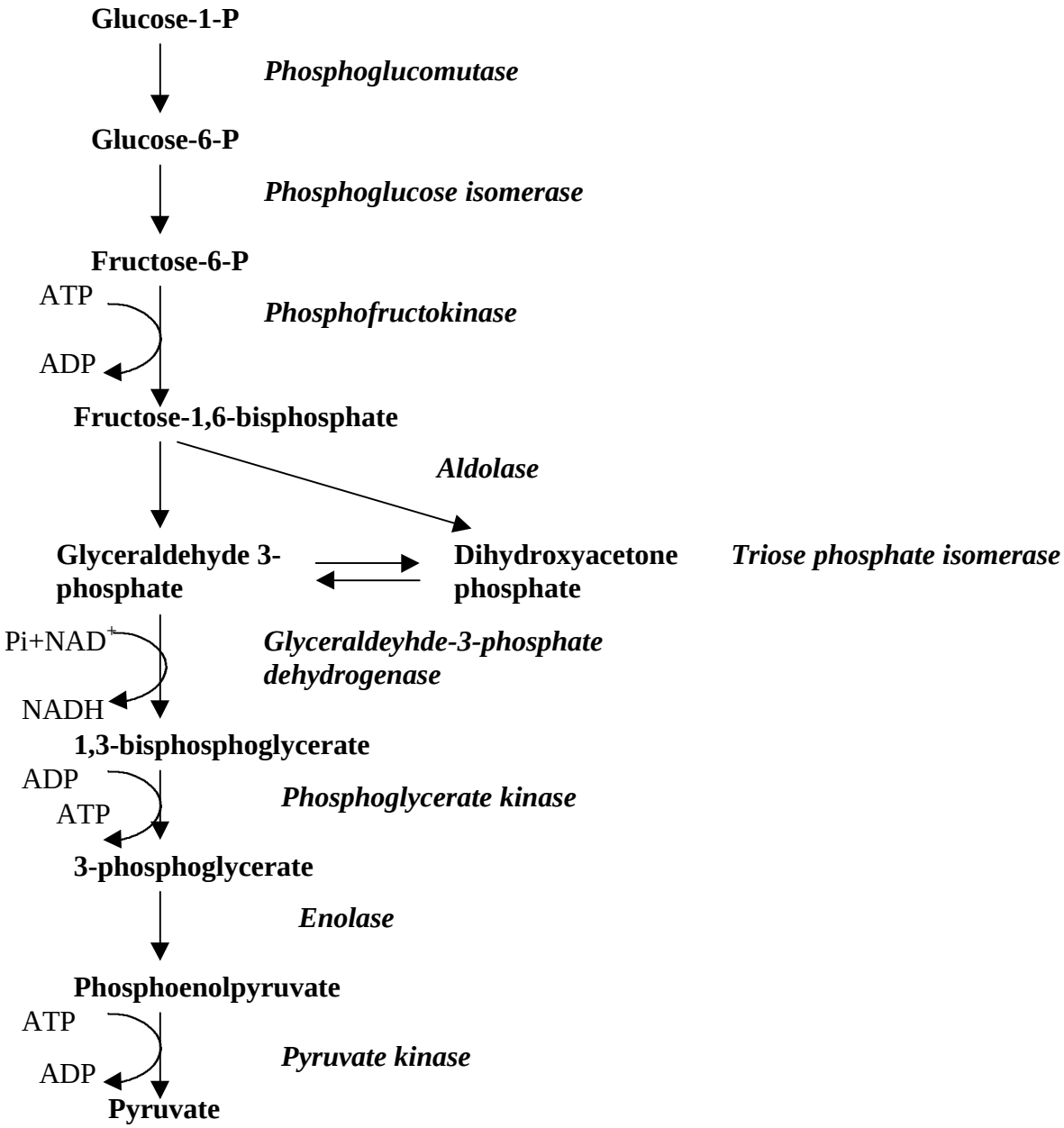

Figure 14. The EMP pathway that was shown to be operative in the anaerobic zones for glycogen degradation at 20°C and 5°C.

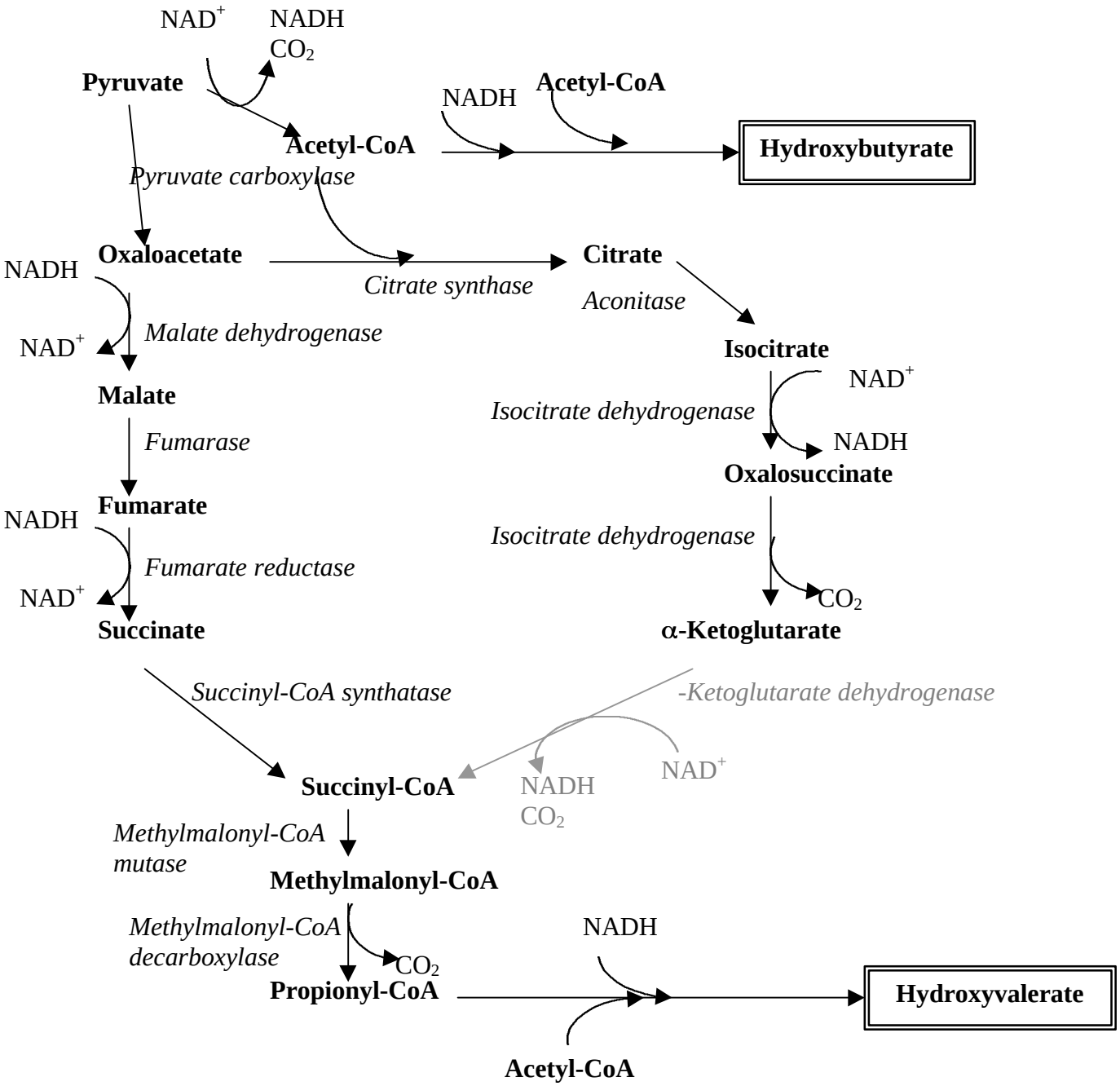

Figure 15. The branched TCA cycle of EBPR anaerobic metabolism that was shown to be operating at 20°C. α-Ketoglutarate dehydrogenase activity ceases when TCA cycle is branched.

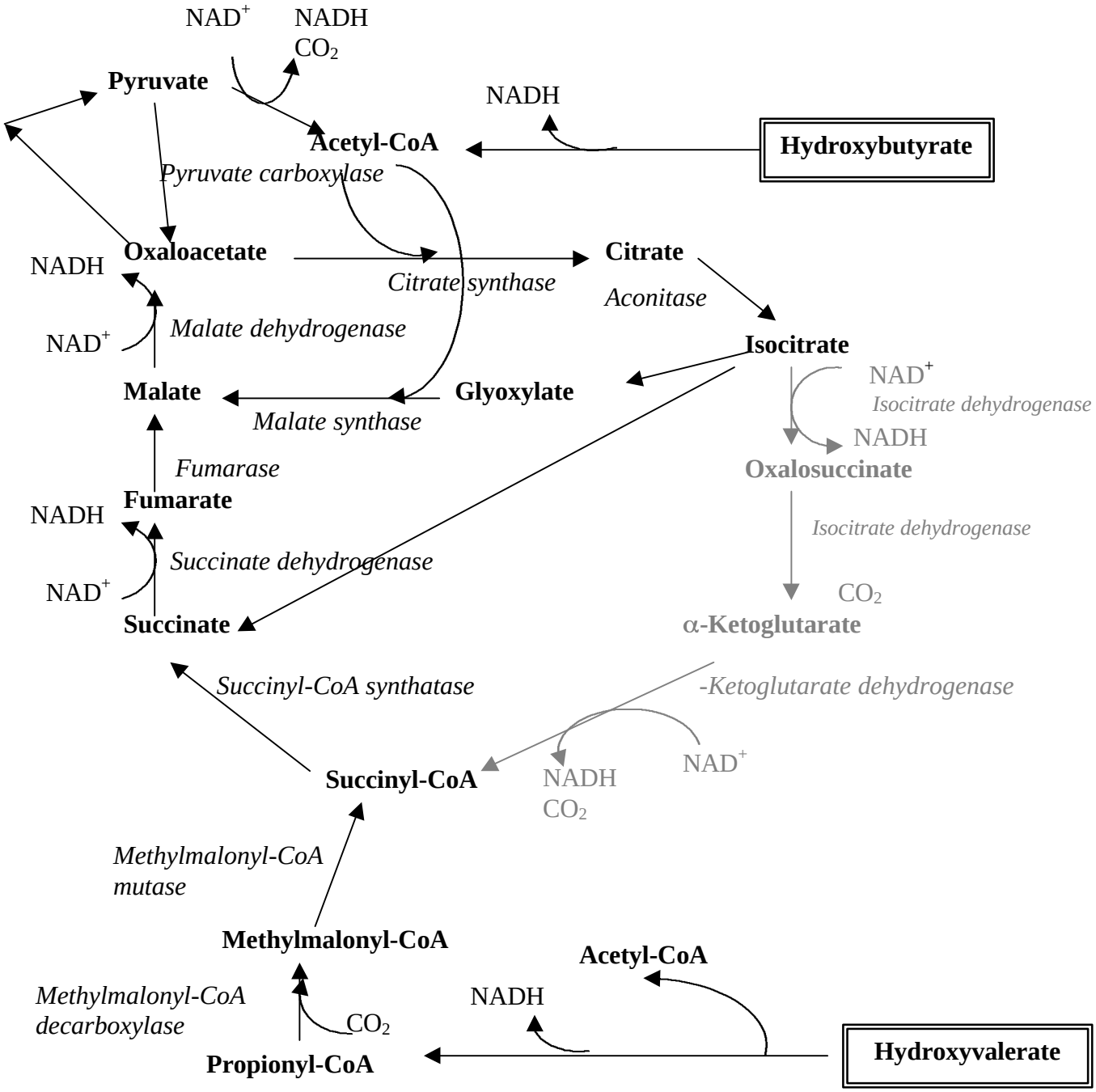

Figure 16. Aerobic metabolism of EBPR sludge that involves glyoxylate cycle at 20°C. Faint colored reactions belong to the TCA cycle and they are presumed be inoperative.

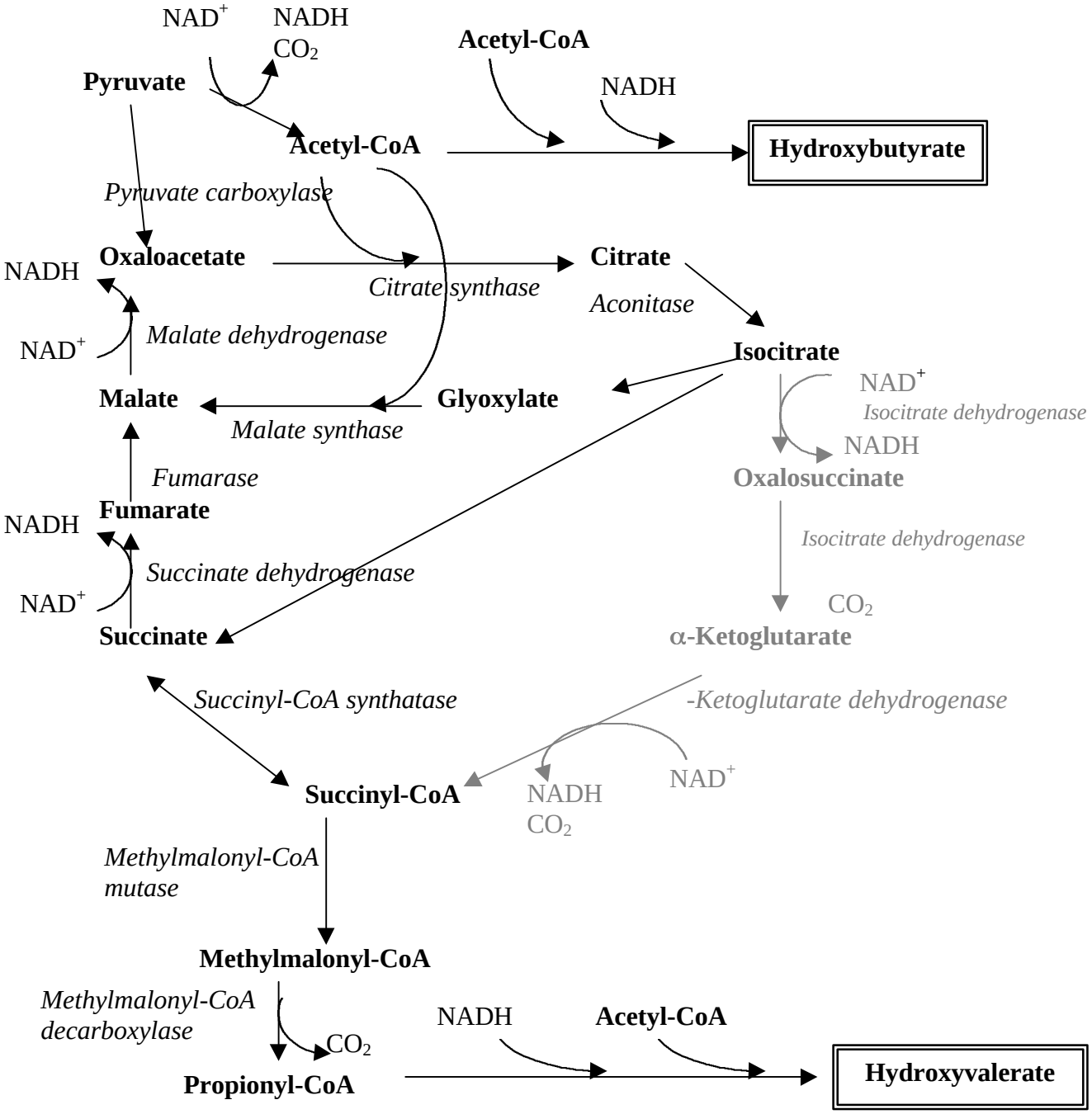

Figure 17. Anaerobic metabolism of EBPR biomass operating at 5°C.

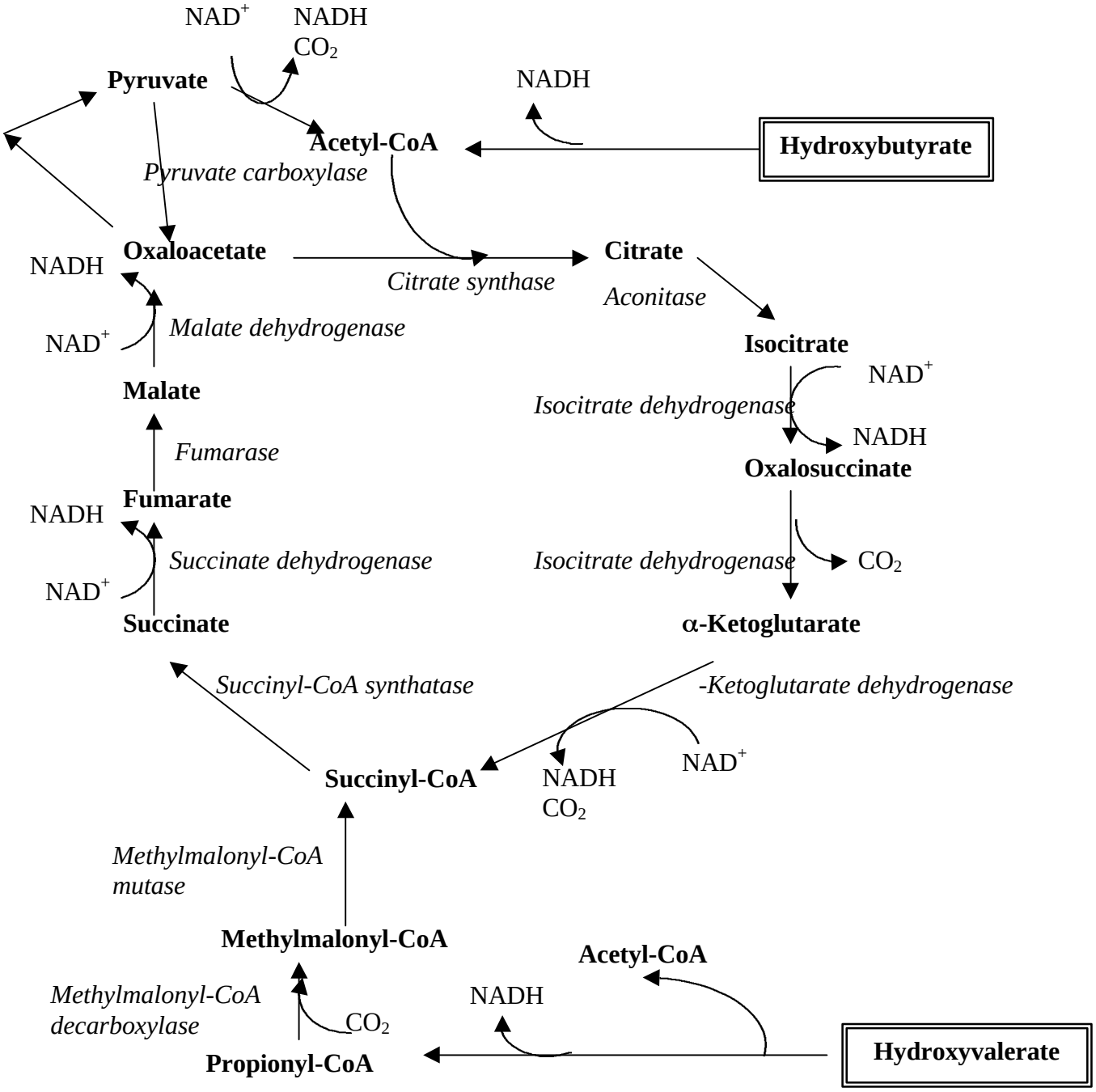

Figure 18. TCA cycle proposed to be used for PHA oxidation at 5°C

CONCLUSIONS

Following an extensive investigation of the EBPR metabolisms that included determination of system performance under two different temperature conditions and detailed enzymatic and molecular work (NMR analysis of intracellular storage products) the EBPR metabolism was shown to exhibit different responses under different conditions. Although an effective inhibitor of the glycogen phosphorylase metabolism was not found for activated sludge samples, cold temperature stress proved to be a useful tool for investigating metabolic pathways active in EBPR biomasses. One thing that needs to be kept in mind is that the biomass under study was strongly enriched with a robust poly-P population, which was demonstrated during the U. Erdal (2002) study when he attempted to wash out the phosphorus removing population. Results of that study showed that as long as there are sufficient poly-P stores that can be used for energy requirements, PAOs can survive down to a total SRT value of 3.5 days (2.1 d aerobic SRT) even at 5°C, until the glycogen replenishment becomes limiting.

The two EBPR biomasses maintained at 20 and 5°C showed major metabolic differences whereby they maintain their energy and reducing equivalents balances. The results of this study fill an important gap in EBPR research by providing enzymatic proof of the activity of the proposed metabolisms. At 20°C the microbial population was shown to utilize the glyoxylate cycle under aerobic conditions, which helps them conserve carbons and reducing equivalents that are needed for glycogen synthesis. Under cold temperature conditions, on the other hand, the EBPR sludge was shown to utilize the glyoxylate cycle under anaerobic conditions instead of the branched TCA pathway. This is possibly due to a less strict need to consume excess NADH generated during glycogen degradation. Another reason of such a shift can be the need for extra reducing equivalents when the amount provided from glycolysis is insufficient. Because of kinetic limitations, glycogen degradation was shown to operate even slower at cold temperatures. The slowed kinetics then lead to a decreased use of glycogen at 5°C, closing the gap between the need and production of NADH under anaerobic conditions.

Under anaerobic conditions at 5°C, the relative activities of succinate dehydrogenase and succinyl-CoA synthatase enzymes determine the distribution of succinate between fumarate and succinyl-CoA. The production of hydroxyvalerate units of the PHA polymer necessitates a relatively higher succinyl-CoA synthatase activity in order to remove succinate from the glyoxylate shunt. Such partitioning of succinate will also impact the amount of reducing equivalents produced in the system, since when the succinate dehydrogenase activity is significantly lowered, production of 1 reducing equivalent ($FADH_2$, or NADH) will be lost. The organisms would then need to use the shunt, or other mechanisms not investigated in this study in order to be able to produce sufficient amounts of reducing equivalents for PHA synthesis. It was also observed that especially at cold temperatures, poly-P organisms gain advantage over the non-poly-P organisms. This can be explained by their ability to alter their metabolism. Also, their readily available energy source, poly-P, gives them rapid access to ATP for activation of acetate to acetyl-CoA, whereas the non-poly-P organisms need to generate ATP through multi-step metabolic processes eventually slowing down the rate of substrate uptake even at 20°C.

The practical implications of this research will be significant, since the computer models used in actual design practice are based on earlier biochemical models developed for EBPR sludges. The results presented in this study show that, based on the environmental conditions, organisms responsible from EBPR have the capability to alter their biochemical metabolism based on the environmental conditions. Therefore, design assumptions made based on one environmental condition would not fit to another. For example, it is not possible to assume unchanged glycogen involvement under changing temperature conditions, or decreased phosphorus removal at low temperatures just because the kinetics of the biochemical reactions slow down.

REFERENCES

Akitt, J.W. (1992) NMR and Chemistry: an Introduction to Modern NMR Spectroscopy. Chapman & Hall. London-New York.

Atherton, N.M. (1993) Principles of Electron Spin Resonance. Ellis Horwood, PTR Prentice Hall, Great Britain.

Barham, P.J.; Barker, P. and Organ, S.J. (1992) Physical properties of poly9hydroxybutyrate) and copolymers of hydroxybutyrate and hydroxyvalerate. *FEMS Micro. Rev*. **103** 289-298.

Barnard, G.N. and Sanders, J.K.M. (1989) The poly(β-hydroxybutyrate) granule in vivo. *J. Biol. Chem*. **6** 3286-3291.

Beer, D. and Vasella, A. (1985) Aldonohydroxymo-lactones: Preparation and determination of configuration. *Helvetica Chimica Acta*. **68** 2254-2274.

Bergmeyer, H. U.; Bergmeyer, J. and Graßl, M. (1983) *Metods of Enzymatic Analysis*. Vol. I, II, III. 3rd Ed. Verlag Chemie. Weinheim, Germany.

Berliner, L.J. and Reuben, J. (1992) Biological Magnetic Resonance. v.10. Carbohydrates and Nucleic Acids. Plenum Press, New York.

Bermudez, O.; Padilla, P.; Huitron, C. and Flores, M. E. (1998) Influence of carbon and nitrogen source on synthesis of NADP+-isocitrate dehydrogenase, methylmalonyl-coenzyme A mutase, and methylmalonyl-coenzyme A decarboxylase in *Saccharopolyspora erythraea* CA340. *FEMS Micro. Let*. **164** 77-82.

Bollen, M. and Stalmans, W. (1989) The antiglycogenolytic action of 1-deoxynojirimycin results from a specific inhibition of the α-1,6-glucosidase activity of the debranching enzyme. *Eur. J. Biochem*. **181** 775-780.

Brdjanovic, D., Slamet, A., van Loodsdrecht, M.C.M., Hooijmans, C.M., Alaerts, G.J. and Heijnen, J.J. (1998) Impact of excessive aeration on biological phosphorus removal from wastewater. *Wat. Res*. **32**(10) 200-208.

Carucci, A.; Lindrea, K.; Majone, M. and Ramadori, R. (1999) Different mechanisms for the anaerobic storage of organic substrates and their effect on enhanced biological phosphate removal (EBPR). *Wat. Sci. Tech*. **39** (6) 21-28.

Christensson, M., Blackall, L.L. and Welander, T. (1998) Metabolic transformations and characterization of the sludge community in an enhanced biological phosphorus removal system. *Appl. Microbial Biotech*. **49** 226-234

Comeau, Y., Hall, K.J., Hancock, R.E.W. and Oldham, W.K. (1986) Biochemical Model for enhanced biological phosphorus removal. *Wat. Res*. **20** (12) 1511-1521.

Comeau, Y., Oldham, W.K. and Hall, K.J. (1987) Dynamics of carbon reserves in biological dephosphatation of wastewater. *Proc. of IAWPRC Specialized Conference*, 28-30 Sept. 1987. Rome. Italy. 39-55.

Cowan, B. (1997) *Nuclear Magnetic Resonance and Relaxation*. Cambridge University Press.

Derome, A.E. (1987) *Modern NMR Techniques for Chemistry Research*. Pergamon Press, Oxford- New York.

Dixon and Kornberg (1959) Assay methods for key enzymes of the glyoxylate cycle. *Biochem. J*. **72** 3.

Doi, Y. (1990) *Microbial polyesters*. VCH. New York

Dringen, R. and Hemprecht, B. (1993) Inhibition by 2-deoxyglucose and 1,5-gluconolactone of glycogen mobilization in astroglia-rich primary cultures. *J. Neurochem.* **60** (4) 1498-1504.

Erdal, Z.K. and Randall, C.W. (2002a) An Investigation of the Biochemistry of Biological Phosphorus Removal Systems: Literature Review. PhD Dissertation. Virginia Polytechnic Institute and State University. Blacksburg, Virginia.

Erdal, Z.K. and Randall, C.W. (2002b) An Investigation of the Biochemistry of Biological Phosphorus Removal Systems: Impact of the Feed COD/TP Ratio on the Intracellular Storage Materials and System Performance of Biological Phosphorus Removal. PhD Dissertation. Virginia Polytechnic Institute and State University. Blacksburg, Virginia.

Erdal, U.G. (2002) *The Effects of Temperature on System Performance and Bacterial Community Structure in a Biological Phosphorus Removal System*. PhD Dissertation. Virginia Polytechnic Institute and State University, Blacksburg, Virginia.

Ernest, M.J. and Kim, K.K. (1973) Regulation of rat liver glycogen synthetase. *J. Biol. Chem*. **248** (5) 1550-1555.

Gerhadt, P.; Murray, R.G.E.; Wood, W.A. and Krieg, N. R. (1995) *Methods for General and Molecular Bacteriology*. American Society for Microbiology. Washington, DC.

Gunther, H. (1995) *NMR Spectroscopy: basic Principles, Concepts, and Applications in Chemistry*. John Wiley and Sons, Chichester-New York.

Hesselmann, R.P.X.; von Rummell, R.; Resnick, S.M.; Hany, R. and Zehnder, A.J.B. (2000) Anaerobic metabolism of bacteria performing enhanced biological phosphate removal. *Wat. Res*. **34** (14) 3487-3494.

Kuby, S.A. (1991) *A Study of Enzymes*. CRC Press. Boca Raton.

Kuschel, P.W. (1989) Biological applications of NMR. In *Analytical NMR*. John Wiley and Sons. 159-212.

Lai, J.C.K. and Cooper, A.J.L. (1986) Brain α-ketoglutarate dehydrogenase complex: kinetic properties, regional distribution, and effects of inhibitors. *J. Neurochem*. **47** 1376-1386.

Lau, K.H. and Thomas, J. A. (1983) Specific mixed disulfide formation with purified bovine cardiac glycogen synthase I and glutathione. *J. Biological Chemistry.* **258** (4) 2321-2326.

Lauzier, C.; Revol, J.F. and Marchessault, R.H. (1992) Topotactic crystallization of isolated poly(β-hydroxybutyrate) granules from *Alcaligenes eutrophus*. *FEMS Micro. Rev*. **103** 299-310.

Lemire, B. D. and Weiner, J. H. (1986) Fumarate Reductase of *Escherichia coli*. In *Methods in Enzymology*, eds. Fleischer, S. and Fleischer, B. v.**126**. 377-386.

Liu, W., Mino, T., Nakamura, K. and Matsuo, T. (1996) Glycogen accumulating population and its anaerobic substrate uptake in anaerobic-aerobic activated sludge without biological phosphorus removal. *Wat. Res.* **30** (1) 75-82.

Louie, T.M., Mah, T.J., Oldham, W. and Ramey, W.D. (2000) Use of metabolic inhibitors and gas chromatography / mass spectrometry to study poly-β-hydroxyalkanoates metabolism involving cryptic nutrients in enhanced biological phosphorus removal systems. *Wat. Res*. **34**(5) 1507-1514.

Martin, J.L. *et al*. (1991) Glucose analogue inhibitors of glycogen phosphorylase: the design of potential drugs for diabetes. *Biochem*. **30** 10101-10116.

Maurer, M., Gujer, W., Hany, R. and Bachman, S. (1997) Intracellular carbon flow in phosphorus accumulating organisms from activated sludge systems. . *Wat. Res*. **31**(4) 907-917.

Mino, T., Arun, V., Tsuzuki, Y. and Matsuo, T. (1987) Effect of phosphorus accumulation on acetate metabolism in the biological phosphorus removal process. *Proc. of IAWPRC Specialized Conference*, 28-30 Sept. 1987. Rome. Italy. 27-38.

Moat, A.G. and Foster, J. W. (1995) *Microbial Physiology*. John Wiley and Sons, Inc. New York, NY.

Monori, B.M.; Kubicek, C.P.; Habison, A.; Kubicek, E.M. and Rohr, M. (1985) Presence and regulation of the α-ketoglutarate dehydrogenase multienzyme complex in the filamentous fungus *Aspergillus niger*. *J. Bacteriol*. **161** (1) 265-271.

Niitsu, Y.; Hori, O.; Yamaguchi, A.; Bando, Y.; Ozawa, K.; Tamatani, M.; Ogawa, S. and Tohyama, M. (1999) Exposure of cultured primary rat astrocytes to hypoxia results in intracellular glucose depletion and induction of glycolytic enzymes. *Molecular Brain Research.* **74** (1-2) 26-34.

Papageorgiou, A.C.; Oikonomakos, N.G. and Leonidas, D.D. (1989) Inhibition of rabbit muscle glycogen phosphorylase by d-gluconohydroximo-1,5-lactone-N-phenylurethane. *Arch. Biochem. Bioph.* **272** (2) 376-385.

Paudler, W.W. (1987) *Nuclear Magnetic Resonance*. John Wiley and Sons. USA.

Pereira, H., Lemos, P.C., Reis, M.A.M., Crespo, J.P.S.G., Carrondo, M.J.T. and Santos, H. (1996) Model for carbon metabolism in biological phophorus removal processes based on *in vivo* ^{13}C-NMR labeling experiments. *Wat. Res.* **30**(9) 2128-2138.

Popov, V. N. *et al.* (1998) *FEBS Let.* **440** 55-58.

Popov, V. N.; Igamberdiev, A. U.; Schnarrenberger, C. and Volvekin, S. V. (1996) Induction of glyoxylate cycle enzymes in rat liver upon food starvation. *FEBS Let*. **390** 258-260.

Punrattanasin, W. (2001) *The Utilization of Activated Sludge Polyhydroxyalkanoates for the Production of Biodegradable Plastics*. PhD Dissertation. Virginia Polytechnic Institute and State University, Blacksburg, Virginia.

Saier, M. H. (1987) *Enzymes in Metabolic Pathways*. Harper Press. New York, NY.

Sanders, J.K.M. and Hunter, B.K. (1993) *Modern NMR Spectroscopy: A Guide for Chemists*. Oxford University Press. New York.

Serrano, J. A.; Camacho, M. and Bonete, M.J. (1998) Operation of glyoxylate cycle in halophilic archaea: presence of malate synthase and isocitrate lyase in *Haloferax volcanii*. *FEBS Let*. **434** 13-16.

Shimazu, T.; Tokutake, S. and Usami, M. (1978) Inactivation of phosphorylase phosphatase by a factor from rabbit liver and its chemical characterization as glutathione disulfide. *J. Biol. Chem*. **253** (20) 7376-7382.

Silverman, R.B. (2000) *The Organic Chemistry Of Enzyme-Catalyzed Reactions.* Academic Press. London.

UNITIKA Enzymes Ltd., Medical Development Department, Technical Development Division. Osaka, Japan.

Watson, K.A.; Mitchell, E.P.; Johnson, L.N.; Son, J.C.; Bichard, C.J.; Orchard, M.G.; Fleet, G.W.; Oikonomakos, N.G.; Leonidas, D.D. and Kontou, M. (1994) Design of inhibitors of glycogen phosphorylase: a study of alpha- and beta-C-glucosides and 1-thio-beta-D-glucose compounds. *Biochem*. **33** (19) 5745-5758.

Wentzel, M.C.; Lotter, L. H.; Ekama, G.A.; Loewenthal, T.E. and Marais, G.v.R. (1991) Evaluation of biochemical models for biological excess phosphorus removal systems – a review. *Wat. Sci. Tech*. **25** 59-82.

White, D. (1995) *Physiology and Biochemistry of Prokaryotes*. Oxford University Press. New York, NY.